PAPER • OPEN ACCESS

Classification of engineered topological superconductors

To cite this article: Panagiotis Kotetes 2013 *New J. Phys.* **15** 105027

View the article online for updates and enhancements.

Related content

- Majorana fermions in semiconductor nanowires: fundamentals, modeling, and experiment
  T D Stanescu and S Tewari

- Interplay of topological phases in magnetic adatom-chains on top of a Rashba superconducting surface
  Andreas Heimes, Daniel Mendler and Panagiotis Kotetes

- New directions in the pursuit of Majorana fermions in solid state systems
  Jason Alicea

Recent citations

- Magnetic manipulation of topological states in p-wave superconductors
  Maria Teresa Mercaldo et al

- Magnetic-field-induced topological reorganization of ap-wave superconductor
  Maria Teresa Mercaldo et al

- Synthesizing Majorana zero-energy modes in a periodically gated quantum wire
  Mariana Malard et al

New Journal of Physics

Classification of engineered topological superconductors

Panagiotis Kotetes

Institut für Theoretische Festkörperphysik, Karlsruhe Institute of Technology,
D-76128 Karlsruhe, Germany
E-mail: panagiotis.kotetes@kit.edu

Abstract. I perform a complete classification of two-dimensional, quasi-one-dimensional (1D) and 1D topological superconductors which originate from the suitable combination of inhomogeneous Rashba spin–orbit coupling, magnetism and superconductivity. My analysis reveals alternative types of topological superconducting platforms for which Majorana fermions are accessible. Specifically, I observe that for quasi-1D systems with Rashba spin–orbit coupling and time-reversal violating superconductivity, such as for instance due to a finite Josephson current flow, Majorana fermions can emerge *even in the absence* of magnetism. Furthermore, for the classification I also consider situations where additional 'hidden' symmetries emerge, with a significant impact on the topological properties of the system. The latter generally originate from a combination of space group and complex conjugation operations that separately do not leave the Hamiltonian invariant. Finally, I suggest alternative directions in topological quantum computing for systems with additional unitary symmetries.

IOP Institute of Physics ⬧ DEUTSCHE PHYSIKALISCHE GESELLSCHAFT

Contents

1. Introduction

The breakthrough concept of emergent Majorana fermions (MFs) in artificial topological superconducting devices, pioneered by Fu and Kane [1], motivated a number of recent experiments [2, 3] that have already provided the first promising results. The two authors demonstrated that the helical surface states of a three-dimensional topological insulator (TI) [4], with proximity induced superconducting gap Δ, behave as a time-reversal ($\mathcal{T}$) invariant topological superconductor (TSC). When a magnetic field is applied perpendicular to the topological surface, a single MF appears per superconducting vortex. In fact, the latter mechanism had been discussed earlier by Sato [5] in the context of axion-strings. Shortly after Fu–Kane proposal, it was recognized that the catalytic presence of spin–momentum locking could be alternatively provided by spin–orbit interaction, intrinsic to non-centrosymmetric superconductors (SCs) [6] and Rashba semiconductors [7–10]. In the case of a semiconducting wire [9, 10], fabricated for instance by InSb, a Zeeman energy $\mu_\mathrm{s}|\mathcal{B}|$ is sufficient to lead to MFs localized at the edges. The existence of confined and protected edge MFs is crucial for applications in topological quantum computing (TQC) [11, 12]. A pair of MFs defines a topological qubit, which is in principle [13] free from decoherence and protected against noise, in stark contrast to traditional spin [14] and superconducting qubits [15]. Furthermore, edge

IOP Institute of Physics Φ DEUTSCHE PHYSIKALISCHE GESELLSCHAFT

MFs can also give rise to unique transport signatures [16–19], such as the usual [16, 17] or the magnetically controlled [18] 4π-Josephson effect.

In the case of a semiconducting wire [9, 10] with proximity induced superconductivity, the system transits to the topological phase when the criterion $\mu_s|\mathcal{B}| > \sqrt{\mu^2 + |\Delta|^2}$ is satisfied (μ defines the chemical potential). The concomitant requirement of a high Zeeman energy, which also arises in quasi-one-dimensional (1D) multi-channel [20, 21] analogues of [9, 10], can impede the nanofabrication of the device or restrict the possible manipulations on the MFs. In fact, several proposals concerning quantum information processes rely on the application of strong anti-parallel magnetic fields at the nanoscale level [22], something not easily realizable in the laboratory. As an answer to these obstacles alternative types of engineered TSCs have been put forward, which support MFs without the necessary presence of spin–orbit coupling or the application of a magnetic field [23–28]. In most of these proposals, some kind of inhomogeneous magnetic order coexists with intrinsic or proximity induced superconductivity. For some of these models [26, 27] it has been shown that there is a mapping to the case of the semiconducting wire-based TSC mentioned above.

In this paper I present a complete topological classification of low-dimensional TSCs that support MFs and originate from the combined presence of inhomogeneous Rashba spin–orbit coupling $v(\mathbf{r})$, magnetism $\mathbf{M}(\mathbf{r})$ and superconductivity $\Delta(\mathbf{r})$. My primary goal is to shed light on the topological connection between different existing proposals for engineered TSCs and in addition to propose alternative advantageous platforms. For my analysis I will consider two-dimensional (2D), quasi-1D and 1D systems. The quasi-1D case is obtained from the strict 2D case by the inclusion of a confining potential $V(\mathbf{r})$. My study provides new engineered TSCs that are experimentally accessible. Specifically, I demonstrate that for a heterostructure consisting of two coupled single channel Rashba semiconducting wires deposited on top of a Josephson junction fabricated by two conventional SCs, MFs can emerge even in the absence of magnetic fields or any type of inhomogeneous magnetism. In addition, for the classification I examine the effects of dimensionality on the robustness of MFs through separating the systems under investigation into weak and strong engineered TSCs. Furthermore, I illustrate that so far overlooked discrete symmetries, that I shall refer to as 'hidden' symmetries ($\mathcal{O}$), distinguish models previously considered as topologically equivalent. Generally, hidden symmetries can be either unitary or anti-unitary and result from a combination of space group, time-reversal or other internal symmetry operations that when considered separately do not leave the Hamiltonian invariant (e.g. [29–31]). Here I discuss two examples of hidden symmetries: (i) a unitary hidden symmetry resulting from the combination of a reflection and a translation and (ii) an anti-unitary symmetry resulting from the combination of time-reversal and translation operations. Finally, I also discuss new TQC perspectives that appear when additional unitary symmetries, including hidden symmetries, are present.

At this point, I give a brief description of how the several sections are organized. In section 2, I provide a short introduction to MFs and introduce the general Hamiltonian that describes the systems of interest. In section 3, I shortly review the topological classification methods with special focus on the situations where additional unitary and anti-unitary symmetries are present. In section 4, I present an overview of my main results (table 2) concerning the classification of TSCs when all possible spatial symmetries are broken. I further discuss how the emergence of hidden symmetries can modify table 2. In section 5, I provide a detailed analysis and justification of the results presented in section 4. In section 6, I demonstrate that MFs are accessible in heterostructures consisting of conventional SCs in proximity to **A.**

the surface states of a three-dimensional (3D) TI or **B.** two coupled single channel Rashba semiconducting wires, when in both cases a Josephson current is injected to the system. In section 7, I present two specific examples of systems characterized by a hidden symmetry and study the impact of the latter on the topological properties. In section 8, I discuss how the presence of hidden symmetries can be useful for developing TQC protocols and suggest possible candidate systems that could be used for this purpose. Finally, section 9 summarizes my main results and related conclusions.

2. Majorana fermions and model Hamiltonian

In condensed matter physics MFs are not fundamental particles [32] but excitations of a many-body system [33, 34]. Essentially, what we define as MFs are the operators γ_α (α is just a label) which satisfy $\{\gamma_\alpha, \gamma_\beta\} = \delta_{\alpha,\beta} I$ (I the identity operator) and constitute zero energy eigenoperators of the Bogoliubov–de Gennes (BdG) Hamiltonian. Since MFs are Hermitian they can be described by the following general expression:

$$\gamma_\alpha = \int \mathrm{d}\boldsymbol{r} \left[u^*_{\uparrow,\alpha}(\boldsymbol{r}) \psi_\uparrow(\boldsymbol{r}) + u^*_{\downarrow,\alpha}(\boldsymbol{r}) \psi_\downarrow(\boldsymbol{r}) + u_{\uparrow,\alpha}(\boldsymbol{r}) \psi^\dagger_\uparrow(\boldsymbol{r}) + u_{\downarrow,\alpha}(\boldsymbol{r}) \psi^\dagger_\downarrow(\boldsymbol{r}) \right], \quad (1)$$

where $\psi^\dagger_\sigma(\boldsymbol{r})/\psi_\sigma(\boldsymbol{r})$ correspond to the creation/annihilation operators of an electron with position vector $\boldsymbol{r}$ (here $\boldsymbol{r} = (x, y)$) and spin projection $\sigma = \uparrow, \downarrow$. Notice that MFs require linear combinations of electronic operators and their Hermitian conjugates. Consequently, in order for MFs to constitute the only type of accessible eigen-operators of the single-particle Hamiltonian, we have to restrict ourselves to systems in which the spin-quantization axis is fixed. Notice that for a system with spin-rotational symmetry, the application of a homogeneous magnetic field breaks the latter symmetry but the spin-quantization axis can always be redefined. In this case, MFs are not accessible *directly*, but only as constituent operators of electronic eigen-operators. As a matter of fact, MFs can fundamentally appear only in systems with spin–orbit coupling, spin-triplet superconductivity or magnetism with spatially dependent polarization.

In this work I focus on systems that satisfy the above requirements and are either microscopically or phenomenologically (for heterostructures) described by the following Hamiltonian:

$$\mathcal{H} = \int \mathrm{d}\boldsymbol{r}\, \hat{\psi}^\dagger(\boldsymbol{r}) \left[\frac{\hat{\boldsymbol{p}}^2}{2m} - \mu + V(\boldsymbol{r}) - \boldsymbol{M}(\boldsymbol{r}) \cdot \boldsymbol{\sigma} + \frac{\{v(\boldsymbol{r}), \hat{p}_x \sigma_y - \hat{p}_y \sigma_x\}}{2} \right] \hat{\psi}(\boldsymbol{r})$$

$$+ \int \mathrm{d}\boldsymbol{r} \left[\psi^\dagger_\uparrow(\boldsymbol{r}) \Delta(\boldsymbol{r}) \psi^\dagger_\downarrow(\boldsymbol{r}) + \psi_\downarrow(\boldsymbol{r}) \Delta^*(\boldsymbol{r}) \psi_\uparrow(\boldsymbol{r}) \right], \quad (2)$$

where $\hat{\psi}^\dagger(\boldsymbol{r}) = (\psi^\dagger_\uparrow(\boldsymbol{r})\ \psi^\dagger_\downarrow(\boldsymbol{r}))$, $\boldsymbol{\sigma}$ are the spin Pauli matrices, $v(\boldsymbol{r})$ is the spatially dependent strength of the Rashba spin–orbit coupling, $\boldsymbol{M}(\boldsymbol{r})$ corresponds to a magnetic field or a magnetization profile and $\Delta(\boldsymbol{r})$ defines a spatially varying superconducting order parameter. Notice that in some sense the above Hamiltonian is overcomplete, since it covers all the cases that we will consider, without implying that all the terms are simultaneously required for obtaining a TSC. Furthermore, at the level of my topological classification, the origin of the involved terms is unimportant. However, I have to remark that when I will discuss specific cases I will concentrate on engineered TSCs, which for instance involve conventional types of

magnetism and mainly proximity induced superconductivity [35]. This implies that I will not consider here the cases of unconventional[1] density waves [36–40] or SCs [41], although some of the conclusions could also be applied to these systems.

Since for the situations considered in the present study the spin-quantization is always fixed, I will employ the following spinor:

$$\widehat{\Psi}^{\dagger}(\boldsymbol{r}) = \left(\psi_{\uparrow}^{\dagger}(\boldsymbol{r}), \psi_{\downarrow}^{\dagger}(\boldsymbol{r}), \psi_{\uparrow}(\boldsymbol{r}), \psi_{\downarrow}(\boldsymbol{r}) \right), \tag{3}$$

and use the $\boldsymbol{\tau}$ Pauli matrices in order to represent matrices in the Nambu particle–hole space. With the introduction of the above enlarged spinor the Hamiltonian can be rewritten in the following compact way:

$$\mathcal{H} = \frac{1}{2} \int d\boldsymbol{r} \ \widehat{\Psi}^{\dagger}(\boldsymbol{r}) \widehat{\mathcal{H}}(\hat{\boldsymbol{p}}, \boldsymbol{r}) \widehat{\Psi}(\boldsymbol{r}), \tag{4}$$

where $\widehat{\mathcal{H}}(\hat{\boldsymbol{p}}, \boldsymbol{r})$ corresponds to the BdG Hamiltonian. Notice that the factor of $1/2$ is crucial for avoiding double counting of the degrees of freedom, since the above spinor does not obey to the usual fermionic commutation relations.

3. Topological classification principles

Before discussing the possible topological phases arising from our model Hamiltonian, I will briefly review the basics of how to classify topological systems. My goal is to first highlight a key point which is crucial for classifying TSCs and then demonstrate how this can provide further topological insight concerning previously studied systems [26, 27]. This key point is that topological classification of systems following the recently developed methods [42–44], is conducted for irreducible Hamiltonians, for which one cannot find any unitary operator $\mathcal{O}_{\mathrm{u}}$ satisfying $[\widehat{\mathcal{H}}(\hat{\boldsymbol{p}}, \boldsymbol{r}), \mathcal{O}_{\mathrm{u}}] = 0$. If there is a number of these type of operators, we can block diagonalize the Hamiltonian and topologically classify each sub-block. Of course, this is not the only route to study topological properties, since one can also directly construct topological invariants for reducible Hamiltonians [45]. Nevertheless, studying irreducible Hamiltonians provides a transparent analysis of the topological classes.

The symmetry class and the related accessible topological phases of an irreducible Hamiltonian are defined by the possible presence of three specific types of discrete symmetries. The first two correspond to a generalized time-reversal symmetry effected by the anti-unitary operator Θ and a charge conjugation symmetry effected by an anti-unitary operator Ξ. If Θ is a symmetry of the Hamiltonian, it satisfies $[\widehat{\mathcal{H}}(\hat{\boldsymbol{p}}, \boldsymbol{r}), \Theta] = 0 \Rightarrow \Theta^{-1}\widehat{\mathcal{H}}(\hat{\boldsymbol{p}}, \boldsymbol{r})\Theta = +\widehat{\mathcal{H}}(\hat{\boldsymbol{p}}, \boldsymbol{r})$ while in the case of charge-conjugation we instead have $\{\widehat{\mathcal{H}}(\hat{\boldsymbol{p}}, \boldsymbol{r}), \Xi\} = 0 \Rightarrow \Xi^{-1}\widehat{\mathcal{H}}(\hat{\boldsymbol{p}}, \boldsymbol{r})\Xi = -\widehat{\mathcal{H}}(\hat{\boldsymbol{p}}, \boldsymbol{r})$. If Θ and Ξ constitute symmetries of the Hamiltonian at the same time, then the Hamiltonian additionally satisfies $\{\widehat{\mathcal{H}}(\hat{\boldsymbol{p}}, \boldsymbol{r}), \Theta\Xi\} = 0$ where the combined $\Theta\Xi$ operator is unitary and is termed chiral symmetry operator Π. The inclusion of Π completes the set of symmetries that are required for determining the symmetry class of an irreducible Hamiltonian. In fact, in order to cover all possible symmetry classes, we have to take into account the case in which a unitary chiral symmetry may exist without the necessary presence of Θ and Ξ symmetries.

---

[1] Here, the characterization 'unconventional' is assigned to order parameters of density wave or superconducting phases, that carry finite angular momentum such as p-wave, d-wave, etc.

Table 1. Symmetry classes of topological SCs supporting MFs '*fundamentally*', i.e. the eigen-operators diagonalizing the single-particle Hamiltonian are solely of Majorana type. For Θ and Ξ, $\pm I$ corresponds to the result of Θ^2 and Ξ^2. For Π, I denotes that the symmetry is present. Conversely, 0 implies that the corresponding symmetry is broken.

Class	Θ	Ξ	Π	1D	2D	3D
BDI	$+I$	$+I$	I	$\mathbb{Z}$	0	0
D	0	$+I$	0	$\mathbb{Z}_2$	$\mathbb{Z}$	0
DIII	$-I$	$+I$	I	$\mathbb{Z}_2$	$\mathbb{Z}_2$	$\mathbb{Z}$

Another important aspect which has not been pointed out so far in the existing classification schemes, concerns correlated systems and the role of induced order parameters [46–49] on the topological properties of a system. Within a mean-field description, it has been shown that there exist patterns [47, 49] of thermodynamic phases and their corresponding order parameters, which are bound to coexist at a microscopic level. In fact, Varelogiannis [49], recently put forward a rule according to which one can predict the induced order parameters and consequently the complete patterns of thermodynamic/topological phases which can be decomposed in fundamental coexistence quartets of phases. Although the symmetry properties of an induced order parameter is strictly determined by the already existing order parameters and consequently cannot alter the symmetry class, its inclusion can deform the topological phase diagram by modifying the parameter regime for observing the accessible topological classes.

In this work I am interested in 'hidden' unitary discrete symmetry operators satisfying the property $\mathcal{O}_u^n = I$, with $n \in \mathbb{Z}$. In the simplest case $n = 2$, we can block diagonalize the Hamiltonian into two sub-blocks labelled by the eigenvalues ± 1 of $\mathcal{O}_u$, leading to a direct sum of the form $\widehat{\mathcal{H}}_+(\hat{p}, r) \oplus \widehat{\mathcal{H}}_-(\hat{p}, r)$. Notice that because of the discrete symmetry $\mathcal{O}_u$, both sub-blocks are constrained to belong to the same symmetry class. However, the two sub-systems do not necessarily reside in the same topological class. In addition, I also provide an example of an anti-unitary hidden symmetry $\mathcal{O}_a$. In this case $\mathcal{O}_a$ constitutes an additional generalized time-reversal symmetry which modifies the initial symmetry class of the system, instead of splitting the latter in a direct sum of identical symmetry classes as for the unitary analogue $\mathcal{O}_u$. For instance, if a system is initially in class D, then the emergence of an anti-unitary hidden symmetry $\mathcal{O}_a$ with $\mathcal{O}_a^2 = +I$ will change its symmetry to class BDI.

For the cases under consideration, the BdG Hamiltonian enjoys a charge-conjugation symmetry $\Xi = \tau_x \mathcal{K}$, where $\mathcal{K}$ defines complex conjugation. Since $\Xi^2 = +I$, we obtain only the following three allowed symmetry classes presented in table 1: BDI, D, DIII or their direct sums BDI $\oplus$ BDI, D $\oplus$ D, DIII $\oplus$ DIII in the presence of a hidden symmetry $\mathcal{O}_u$, with $\mathcal{O}_u^2 = I$. Notice that the classes BDI and DIII are characterized by a time-reversal symmetry Θ with $\Theta^2 = +I$ and $\Theta^2 = -I$, respectively. In the first case, Θ symmetry implies that the Hamiltonian is real while in the second that there exist a Kramers-type degeneracy leading to doublets of solutions. Below I examine the minimal cases that can lead to a symmetry class supporting MFs. For completeness I will also shortly discuss previously studied models.
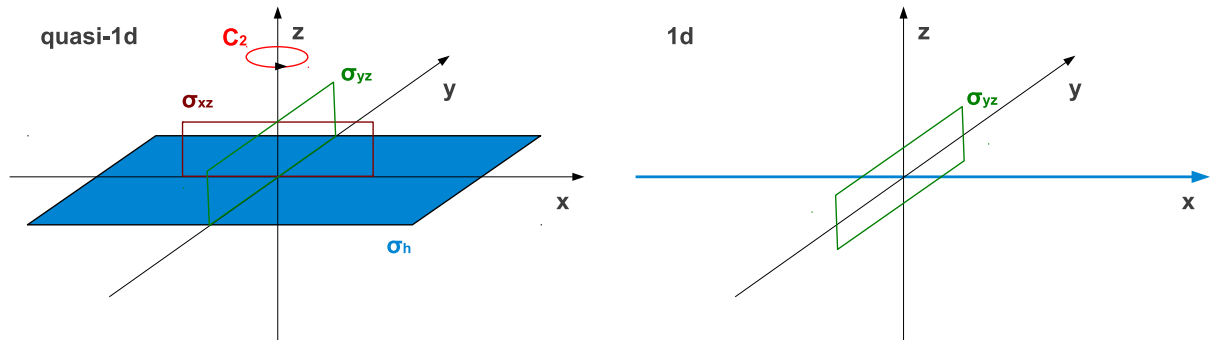
Figure 1. Point group symmetries for quasi-1D and strictly 1D geometries of a topological SC (depicted with blue). In the quasi-1D case, inversion symmetry along the z-axis, σ_h, is broken.

4. Results: possible phases of engineered topological superconductors

In the present section I carry out a thorough analysis of the accessible TSC phases that follow from the Hamiltonian of equation (2). For the strict 2D and 1D cases I will consider that $V(\boldsymbol{r}) = 0$. To analyse the quasi-1D case, I will always assume the presence of a confining potential $V(y)$. For topological computation applications based on edge MFs the quasi-1D and pure 1D setups are the most relevant. The possible unitary symmetries that can appear for these systems originate from the point group $\mathcal{G}$ and translation operations t_a with $t_a \boldsymbol{r} = \boldsymbol{r} + \boldsymbol{a}$. Let me now focus on the point group symmetries for the quasi-1D and pure 1D geometries, which I depict in figure 1. The point group for a quasi-1D system confined in the xy-plane is C_{2v}. This symmetry group includes a C_2 π-rotation about the z-axis ($\boldsymbol{r} \to -\boldsymbol{r}$, $z \to z$) and two σ_v reflection operations σ_{xz} ($y \to -y$) and σ_{yz} ($x \to -x$), where the indices correspond to the mirroring plane. Notice that the reflection symmetry operation $\sigma_h \equiv \sigma_{xy}$ ($z \to -z$) is broken in C_{2v}. In the strict 1D case we are left only with σ_{yz}. For random $v(\boldsymbol{r})$, $\boldsymbol{M}(\boldsymbol{r})$ and $\Delta(\boldsymbol{r})$ all the aforementioned symmetries are broken. Nevertheless, for special spatial profiles of the latter functions, a hidden symmetry can emerge, which consists of these basic symmetry operations or other *already broken* symmetries such as σ_h.

In table 2, I present the topological classification for the Hamiltonian of equation (2) where all possible unitary symmetries are broken due to the spatial dependence of $v(\boldsymbol{r})$, $\boldsymbol{M}(\boldsymbol{r})$ and $\Delta(\boldsymbol{r})$. I demand that $|\boldsymbol{M}(\boldsymbol{r})| \neq 0$ and $|\Delta(\boldsymbol{r})| \neq 0$ so as to avoid any gap closings that could lead to a macroscopic coexistence of different topological phases throughout the volume of the material. I also have to remark that in the case of a translationally invariant system, we can transfer to $\boldsymbol{k}$-space in order to calculate topological invariants. If translational symmetry is broken, then analysis of the topological properties in coordinate or momentum space exhibits the same complexity. Of course, there can be also cases where topological properties in combined $(\boldsymbol{r}, \boldsymbol{k})$-space can be relevant [45, 50].

One of the most important results is case 2 in table 2, where the simultaneous presence of Rashba spin–orbit coupling and inhomogeneous superconductivity can lead to MFs in a quasi-1D system, without the requirement of a magnetic field. In fact, an $\boldsymbol{r}$-dependent superconducting phase originating from a supercurrent falls into this case, constituting an experimentally prominent route towards MFs. As far as the table is concerned, the possible phases are

Table 2. Accessible TSC phases supporting MFs due to the combined presence of inhomogeneous Rashba spin–orbit coupling $v(\boldsymbol{r})$, magnetization $\boldsymbol{M}(\boldsymbol{r})$ and superconducting order parameter $\Delta(\boldsymbol{r})$. The presence (absence) of the aforementioned terms is indicated with $\checkmark$ ($\times$). The resulting symmetry class depends on the behaviour of the magnetic and superconducting Hamiltonian terms under complex conjugation $\mathcal{K}$, since the Rashba spin–orbit coupling term always preserves $\mathcal{T}$. For a term that is already present ($\checkmark$), we denote the case of preserved (broken) complex conjugation as $\mathcal{K} = I$ (0). Notice that symmetry classes that lack a strong topological invariant for the corresponding dimensionality are shown with italics and correspond to weak TSCs. With the phrase '*no-MFs*', I imply that the system belongs to a symmetry class other than D, BDI and DIII, which cannot *fundamentally* support MFs. In the presence of a unitary hidden symmetry $\mathcal{O}_{\mathrm{u}}$ with the property $\mathcal{O}_{\mathrm{u}}^{n} = I$, a symmetry class TC splits into n identical sub-classes $\oplus_{n}$TC. However, the sub-systems do not have to reside in the same topological class. Note that the identification of the symmetry class does not necessarily imply that a system can indeed transit to the topologically non-trivial regime hosting MFs. This depends on the particular implementation.

Case	$v(\boldsymbol{r})$	$\boldsymbol{M}(\boldsymbol{r})$	$\Delta(\boldsymbol{r})$	2D	quasi-1D	1D
I	$\checkmark$	$\times$	$\mathcal{K} = I$	DIII	DIII	*no MFs*
II	$\checkmark$	$\times$	$\mathcal{K} = 0$	D	D	*no MFs*
III	$\times$	$\mathcal{K} = I$	$\mathcal{K} = I$	*BDI*	BDI	BDI
IV	$\times$	$\mathcal{K} = \{0, I, 0\}$	$\mathcal{K} = \{I, 0, 0\}$	D	D	D
V	$\checkmark$	$\mathcal{K} = I$	$\mathcal{K} = I$	D	D	BDI
VI	$\checkmark$	$\mathcal{K} = \{0, I, 0\}$	$\mathcal{K} = \{I, 0, 0\}$	D	D	D

essentially classified by the behaviour of the magnetic and superconducting Hamiltonian terms under $\mathcal{K}$.

5. Analysis of the possible topological phases in the absence of unitary symmetries

In this section I provide the detailed topological classification for the cases presented in table 2. Notice that for the present discussion the spatial dependence of the terms involved is considered random, unless explicitly stated.

5.1. Cases I and II

In the following paragraph I will focus on the cases I and II that are characterized by the presence of inhomogeneous Rashba spin–orbit coupling $v(\boldsymbol{r})$ and superconducting order parameter $\Delta(\boldsymbol{r})$. The TSCs belonging to these cases are described by the following Hamiltonian:

$$\widehat{\mathcal{H}}(\hat{\boldsymbol{p}}, \boldsymbol{r}) = \left[\frac{\hat{\boldsymbol{p}}^2}{2m} - \mu + V(\boldsymbol{r}) \right] \tau_z + \frac{\{v(\boldsymbol{r}), \hat{p}_x \tau_z \sigma_y - \hat{p}_y \sigma_x\}}{2} - \Delta_{\Re}(\boldsymbol{r}) \tau_y \sigma_y - \Delta_{\Im}(\boldsymbol{r}) \tau_x \sigma_y. \tag{5}$$

The Rashba spin–orbit coupling term is odd under inversion symmetry along the z-axis σ_h, while it is even under the usual time-reversal symmetry $\mathcal{T}$. If the superconducting term is also invariant under $\mathcal{T}$ or equivalently $\mathcal{K}$, since we are dealing with a scalar superconducting order parameter, then $\Delta(r) = \Delta_{\Re}(r)$ and the full Hamiltonian is characterized by the generalized time-reversal symmetry $\Theta = i\sigma_y \mathcal{K}$ that coincides with $\mathcal{T}$.

Two-dimensional (2D) system. In the 2D case, the particular system belongs to the symmetry class DIII and is related to the model of [1]. Since Θ satisfies $\Theta^2 = -I$, with I the identity operator, we expect boundary MF Kramers doublets. Class DIII possesses a strong $\mathbb{Z}_2$ topological invariant in 2D. The presence of Θ also leads to a chiral symmetry with $\Pi = \tau_x \sigma_y$. In the case where the superconducting order parameter has an additional imaginary component, $\mathcal{T}$ is broken and the system transits to class D. Class D has a strong $\mathbb{Z}$ invariant in 2D and consequently this system constitutes a strong TSC in both cases.

In order to analyse the symmetry properties in a more transparent manner, I will consider without any loss of generality, the following form for the superconducting order parameter $\Delta(r) = \Delta e^{iJ \cdot r}$. The particular profile, constitutes the simplest representative of $\mathcal{T}$ violating superconductivity and can be viewed either as the result of the spontaneous formation of a Fulde–Ferrell [51] phase with modulation wave-vector J or the consequence of the application of a supercurrent J. The Fulde–Ferrell phase is a special case of pair density waves (see also [52]) that have been also recently considered [24] as potential TSCs leading to MFs. On the other hand, the application of supercurrents was previously discussed in [53]. In the latter implementations a supercurrent was viewed as an additional knob for tuning the topological phase diagram, without though being a necessary ingredient for obtaining a TSC.

At this point we proceed with gauging away the superconducting phase $\varphi(r) = J \cdot r$ via the minimal coupling $\hat{p} \rightarrow \hat{p} + \hbar \nabla \varphi(r) \tau_z / 2 = \hat{p} + \hbar J \tau_z / 2$, leading to

$$\widehat{\mathcal{H}}'(\hat{p}, r) = \frac{\hbar}{2m} J \cdot \hat{p} \, I + \left[\frac{\hat{p}^2}{2m} + \frac{(\hbar J/2)^2}{2m} - \mu + V(r) \right] \tau_z + \frac{\{v(r), \hat{p}_x \tau_z \sigma_y - \hat{p}_y \sigma_x\}}{2} + \frac{v(r)\hbar}{2}$$

$$\times \left(J_x \sigma_y - J_y \tau_z \sigma_x \right) - \Delta \tau_y \sigma_y. \tag{6}$$

It is straightforward to confirm that for $J=0$ the system belongs to class DIII because $\mathcal{T}$ is preserved while for finite J the system lies in class D.

Quasi-one-dimensional (1D) system. In order to investigate the quasi-1D and 1D cases I set $v(r) = v(x)$. Furthermore for the quasi-1D case I additionaly switch on a confining potential $V(r) = V(y)$. The presence of the confining potential lowers the symmetry of the system, permitting anisotropic coefficients for the Rashba terms $\hat{p}_x \tau_z \sigma_y$ and $\hat{p}_y \sigma_x$, instead of a common $v(x)$. For my analysis I will keep the coefficients equal since the only crucial requirement for my study is that they are both non-zero. To achieve confinement, I consider the case of a harmonic potential $V(y) = m\omega^2 y^2 / 2$. This term is translationally invariant along the x-direction and even under C_2, σ_{xz} and σ_{yz}. Another option for the confining potential is the infinite wall potential

$V(|y| > L_y) = +\infty$. For the choice of the harmonic confining potential, the Hamiltonian reads

$$\widehat{\mathcal{H}}(\hat{p}_x, x, \hat{a}, \hat{a}^\dagger) = \frac{\hbar}{2m}\left(J_x\hat{p}_x + J_y\sqrt{\frac{m\omega\hbar}{2}}\,\frac{\hat{a}-\hat{a}^\dagger}{i}\right)I + \left[\frac{\hat{p}_x^2}{2m} + \frac{(\hbar J/2)^2}{2m} - \mu + \hbar\omega\left(\hat{a}^\dagger\hat{a} + \frac{1}{2}\right)\right]\tau_z$$

$$+ \frac{\{v(x), \hat{p}_x\}}{2}\,\tau_z\sigma_y - v(x)\sqrt{\frac{m\omega\hbar}{2}}\,\frac{\hat{a}-\hat{a}^\dagger}{i}\sigma_x + \frac{v(x)\hbar}{2}\left(J_x\sigma_y - J_y\tau_z\sigma_x\right) - \Delta\tau_y\sigma_y,$$

$$(7)$$

where I introduced the quantum harmonic oscillator's bosonic creation (annihilation) operator $\hat{a}^\dagger$ ($\hat{a}$). By introducing the eigenfunctions $|n\rangle$ of the number operator $\widehat{N} = \hat{a}^\dagger\hat{a}$, I obtain the matrix Hamiltonian

$$\widehat{\mathcal{H}}(\hat{p}_x, x) = \frac{\hbar}{2m}\left(J_x\hat{p}_x I + J_y\hbar\lambda_y\right) + \left(\frac{\hat{p}_x^2}{2m} - \mu\lambda_z^J\right)\tau_z + \frac{\{v(x), \hat{p}_x\}}{2}\,\tau_z\sigma_y - v(x)\hbar\lambda_y\sigma_x + \frac{v(x)\hbar}{2}$$

$$\times \left(J_x\sigma_y - J_y\tau_z\sigma_x\right) - \Delta\tau_y\sigma_y,$$

$$(8)$$

that is defined in spin, Nambu and $\widehat{N}$ spaces with

$$\langle n|\lambda_z^J|s\rangle = \delta_{n,s}\left[\mu - \frac{(\hbar J/2)^2}{2m} - \hbar\omega\left(n + \frac{1}{2}\right)\right]/\mu \quad \text{and}$$

$$\langle n|\lambda_y|s\rangle = \sqrt{\frac{m\omega}{2\hbar}}\,\frac{\sqrt{n+1}\delta_{n,s-1} - \sqrt{n}\delta_{n,s+1}}{i}.$$

$$(9)$$

Since the form of the Hamiltonian is identical to the 2D case and $\mathcal{K}^{-1}\lambda_y\mathcal{K} = -\lambda_y$ (similarly to $\hat{p}_y$), the quasi-1D model also belongs to the DIII class[2] for $J = 0$ and to class D for $J \neq 0$.

1D system. For studying the strictly 1D system, I apply the dimensional reduction method to the 2D model of equation (6) and set $\hat{p}_y = J_y = 0$, that yields

$$\widehat{\mathcal{H}}'(\hat{p}_x, x) = \frac{\hbar}{2m}\,J_x\hat{p}_x I + \left[\frac{\hat{p}_x^2}{2m} + \frac{(\hbar J_x/2)^2}{2m} - \mu\right]\tau_z + \frac{\{v(x), \hat{p}_x\}}{2}\,\tau_z\sigma_y + \frac{v(x)}{2}\,\hbar J_x\sigma_y - \Delta\tau_y\sigma_y.$$

$$(10)$$

We observe that for this model we retain our freedom to redefine the spin-quantization axis and as a result the above Hamiltonian does not support MFs in a fundamental manner. If we rotate the spin-quantization axis from y to z, we can rewrite the above Hamiltonian using the usual two-component Nambu spinor $\hat{\psi}_N^\dagger(x) = (\psi_\uparrow^\dagger(x), \psi_\downarrow(x))$, since the four-component formalism becomes redundant in this case. In this formalism the eigenoperators are electronic and their decomposition into MF operators can serve as an equivalent but not necessary description. For instance, if $J_x = 0$, the Hamiltonian in the latter formalism belongs to class AIII which is characterized by a $\mathbb{Z}$ topological invariant in 1D. In this case, the system can support zero-energy edge electronic eigenoperators which can be decomposed into edge MFs. In this sense, MFs are not fundamental in the 1D case.

[2] The 2D and quasi-1D systems always belong to the same symmetry class. Here due to some specific spatial dependences of certain parameters, the symmetry of the quasi-1D system can be enhanced, leading to a different symmetry class. However, this is an artefact of the choices made here for simplifying the discussion. It is assumed that we may always add terms in the quasi-1D Hamiltonian which ensures that all the possible unitary symmetries are broken.

5.2. Cases III and IV

In this section I consider TSC phases that do not involve spin–orbit coupling. This implies that at least two components of an inhomogeneous magnetization field must be present in order to lock the spin-quantization axis, since the latter constitutes a prerequisite for obtaining MFs. For this kind of systems, the Hamiltonian reads

$$\widehat{\mathcal{H}}(\hat{\boldsymbol{p}}, \boldsymbol{r}) = \left[\frac{\hat{\boldsymbol{p}}^2}{2m} - \mu + V(\boldsymbol{r})\right]\tau_z - \boldsymbol{M}(\boldsymbol{r}) \cdot \left(\tau_z\sigma_x, \sigma_y, \tau_z\sigma_z\right) - \Delta_{\Re}(\boldsymbol{r})\tau_y\sigma_y - \Delta_{\Im}(\boldsymbol{r})\tau_x\sigma_y. \quad (11)$$

For the specific type of TSCs, the magnetization field $\boldsymbol{M}(\boldsymbol{r})$ is odd under the usual time-reversal symmetry $\mathcal{T}$. However, its behaviour under complex conjugation $\mathcal{K}$ is not fixed. If $M_y(\boldsymbol{r}) = 0$ then $\boldsymbol{M}(\boldsymbol{r})$ preserves $\mathcal{K}$. This leads to the following two possibilities depending also on the behaviour of the superconducting order parameter under $\mathcal{K}$. In the first possibility the magnetic and superconducting terms are simultaneously invariant under $\mathcal{K}$ and a generalized time-reversal symmetry appears with $\Theta = \mathcal{K}$ accompanied by a chiral symmetry $\Pi = \tau_x$.

2D system. In 2D, the system belongs to the BDI class that however is not characterized by a strong topological invariant for this dimensionality. Consequently, the specific system corresponds to a weak TSC, since under special circumstances one could define weak invariants. The second possibility involves the breaking of $\mathcal{K}$ by either one of the terms. In the latter case, the Hamiltonian belongs to class D which has a strong $\mathbb{Z}$ topological invariant in 2D.

Quasi-1D system. For the particular study I will consider for convenience that $\Delta(\boldsymbol{r}) = \Delta e^{i\boldsymbol{J}\cdot\boldsymbol{r}}$. As previously, I gauge away the superconducting phase and obtain the equivalent model

$$\widehat{\mathcal{H}}'(\hat{\boldsymbol{p}}, \hat{\boldsymbol{r}}) = \frac{\hbar}{2m}\,\boldsymbol{J}\cdot\hat{\boldsymbol{p}}\,I + \left[\frac{\hat{\boldsymbol{p}}^2}{2m} + \frac{(\hbar\boldsymbol{J}/2)^2}{2m} - \mu + V(\boldsymbol{r})\right]\tau_z - \boldsymbol{M}(\boldsymbol{r}) \cdot \left(\tau_z\sigma_x, \sigma_y, \tau_z\sigma_z\right) - \Delta\tau_y\sigma_y.$$

$$(12)$$

For effecting confinement I will employ once again a harmonic oscillator's potential $V(y) = m\omega^2 y^2/2$ and we also have $\boldsymbol{M}(\boldsymbol{r}) = \boldsymbol{M}(x, \hat{a} + \hat{a}^\dagger)$. Following the same steps as in cases I and II, I obtain the Hamiltonian

$$\widehat{\mathcal{H}}'(\hat{p}_x, x) = \frac{\hbar}{2m}\left(J_x\hat{p}_x I + J_y\hbar\lambda_y\right) + \left(\frac{\hat{p}_x^2}{2m} - \mu\lambda_z^J\right)\tau_z - \widehat{\boldsymbol{M}}(x) \cdot \left(\tau_z\sigma_x, \sigma_y, \tau_z\sigma_z\right) - \Delta\tau_y\sigma_y, \quad (13)$$

where $\widehat{\boldsymbol{M}}(x)$ is a real matrix defined in $|n\rangle$ space. If $\boldsymbol{J} = \boldsymbol{0}$ and $\widehat{M}_y(x) = 0$, $\mathcal{K}$ is a symmetry of the Hamiltonian and the system belongs to class BDI (see footnote 2). Instead, if $\widehat{M}_y(x) \neq 0$, the system belongs to class D. For the special case where $\boldsymbol{M}(\boldsymbol{r})$ does not depend on the y-coordinate, i.e. $\boldsymbol{M}(\boldsymbol{r}) = \boldsymbol{M}(x)$, $\widehat{\boldsymbol{M}}(\boldsymbol{r})$ becomes diagonal and can be divided into an infinite number of sub-spaces labelled by n yielding

$$\widehat{\mathcal{H}}'_n(\hat{p}_x, x) = \left[\frac{\hat{p}_x^2}{2m} - \mu + \hbar\omega\left(n + \frac{1}{2}\right)\right]\tau_z - \boldsymbol{M}(x) \cdot \left(\tau_z\sigma_x, \sigma_y, \tau_z\sigma_z\right) - \Delta\tau_y\sigma_y, \quad (14)$$

which leads to the total symmetry class $\oplus_n$BDI. If $\boldsymbol{M}(x)$ violates $\mathcal{K}$ we obtain a direct sum $\oplus_n$D. By allowing a finite $\boldsymbol{J}$ we also violate $\mathcal{K}$. Specifically, if $\boldsymbol{J} = (J_x, 0)$, that corresponds to the case $\Delta(\boldsymbol{r}) = \Delta(x)$, the system resides in the class $\oplus_n$D. However, if $\boldsymbol{J} = (0, J_y)$ the system belongs

to class D (see footnote 2), due to the simultaneous presence of λ_y and λ_z^J in the Hamiltonian of equation (13), that do not allow the decomposition in n-sectors. In table 2 the general case where $\boldsymbol{M}$ and Δ depend on both coordinates is presented.

1D system. By dimensional reduction on the Hamiltonian of equation (12) we obtain the following pure 1D model:

$$\widehat{\mathcal{H}}'(\hat{p}_x, x) = \frac{\hbar}{2m} J_x \hat{p}_x I + \left[\frac{\hat{p}_x^2}{2m} + \frac{(\hbar J_x/2)^2}{2m} - \mu \right] \tau_z - \boldsymbol{M}(x) \cdot \left(\tau_z \sigma_x, \sigma_y, \tau_z \sigma_z \right) - \Delta \tau_y \sigma_y. \quad (15)$$

If $M_y(x) = 0$ and $J_x = 0$, $\mathcal{K}$ is conserved and the system belongs to class BDI. Instead, if one of the previous terms is non-zero, the Hamiltonian is not real any more and it falls into symmetry class D [25].

5.3. Cases V and VI

In the last part of this section I complete the possible cases by considering the situation where all the terms of equation (2) are present. The latter equation in combined Nambu and spin spaces reads

$$\widehat{\mathcal{H}}(\hat{\boldsymbol{p}}, \boldsymbol{r}) = \left[\frac{\hat{\boldsymbol{p}}^2}{2m} - \mu + V(\boldsymbol{r}) \right] \tau_z + \frac{\left\{ v(\boldsymbol{r}), \hat{p}_x \tau_z \sigma_y - \hat{p}_y \sigma_x \right\}}{2} - \boldsymbol{M}(\boldsymbol{r}) \cdot \left(\tau_z \sigma_x, \sigma_y, \tau_z \sigma_z \right)$$
$$- \Delta_{\Re}(\boldsymbol{r}) \tau_y \sigma_y - \Delta_{\Im}(\boldsymbol{r}) \tau_x \sigma_y. \quad (16)$$

When magnetism and Rashba spin–orbit coupling coexist, the accessible topological phases constitute an overlap of the previously examined separate cases. Therefore here we will investigate what are the consequences of the addition of magnetism in cases I and II for different dimensionalities. Earlier, we observed that when magnetism is not present, there are two possible scenarios depending on the behaviour of the superconducting order parameter under $\mathcal{K}$.

2D and quasi-1D systems. For the specific cases, if $\Delta(\boldsymbol{r}) = \Delta_{\Re}(\boldsymbol{r})$ the system resides in the symmetry class DIII being invariant under $\mathcal{T}$. If $\boldsymbol{M}(\boldsymbol{r})$ is introduced, $\mathcal{T}$ will be broken and the system will transit to class D. If $\Delta(\boldsymbol{r})$ is complex, the system is already in class D, and consequently the inclusion of magnetism leads to no additional effects.

1D system. For pure 1D systems the presence of a magnetic order is crucial and leads to new TSC phases. The 1D descendant of the above Hamiltonian reads

$$\widehat{\mathcal{H}}(\hat{p}_x, x) = \left(\frac{\hat{p}_x^2}{2m} - \mu \right) \tau_z + \frac{\left\{ v(x), \hat{p}_x \right\}}{2} \tau_z \sigma_y - \boldsymbol{M}(x) \cdot \left(\tau_z \sigma_x, \sigma_y, \tau_z \sigma_z \right)$$
$$- \Delta_{\Re}(x) \tau_y \sigma_y - \Delta_{\Im}(x) \tau_x \sigma_y. \quad (17)$$

From table 2 we immediately observe that no MFs emerge fundamentally in the absence of magnetism. As mentioned earlier, the reason is that the presence of the spin–orbit coupling term $\tau_z \sigma_y$ alone, cannot lock the spin-quantization axis. Nevertheless, the addition of a perpendicular magnetization field remedies this problem and can lead to TSC phases with MFs. If $\Delta(x)$ and $\boldsymbol{M}(x)$ are invariant under $\mathcal{K}$, the Hamiltonian is characterized by a generalized time-reversal

symmetry $\Theta = \mathcal{K}$ and a chiral symmetry $\Pi = \tau_x$ which permits an integer number of MFs per edge [21]. The translationally invariant version of this model

$$\widehat{\mathcal{H}}(\hat{p}_x) = \left(\frac{\hat{p}_x^2}{2m} - \mu\right)\tau_z + v\hat{p}_x\tau_z\sigma_y - \boldsymbol{M}\cdot\left(\tau_z\sigma_x, \sigma_y, \tau_z\sigma_z\right) - \Delta\tau_y\sigma_y \tag{18}$$

corresponds to the celebrated MF-wire proposal [10] which currently under intense experimental investigation [2] and concerns a Rashba semiconducting wire in the presence of a Zeeman field and proximity induced superconductivity. The systems transits to the topologically non-trivial phase when the criterion

$$|\boldsymbol{M}| > \sqrt{\mu^2 + \Delta^2} \tag{19}$$

is satisfied. Finally, if $\Delta_{\Im}(x)$ or (and) $M_y(x) \neq 0$ then $\mathcal{K}$ is broken and the system belongs to class D with a $\mathbb{Z}_2$ invariant allowing for a single MF per edge.

6. Topological superconductivity based on spin–orbit coupling and supercurrents in the absence of magnetism

In case II, I showed that a quasi-1D system characterized by Rashba spin–orbit coupling and $\mathcal{T}$-breaking superconductivity belongs to symmetry class D, which can in principle support MFs, without any kind of magnetism. In this paragraph I explicitly demonstrate that this scenario is feasible and experimentally accessible. Here I will consider a heterostructure consisting of conventional SCs in proximity to **A.** the surface of a 3D TI and **B.** a double-Rashba semiconducting wire setup, which constitutes the simplest example of a quasi-1D semiconductor. In both cases, the additional presence of a finite supercurrent, will be crucial for engineering topological superconductivity.

6.1. Topological superconductor (TSC) in a heterostructure consisting of a topological insulator and conventional SCs

The respective Hamiltonian describing the TI surface states in the presence of induced pairing reads

$$\widehat{\mathcal{H}}(\hat{\boldsymbol{p}}, \boldsymbol{r}) = -\mu\tau_z + v\left(\hat{p}_x\tau_z\sigma_y - \hat{p}_y\sigma_x\right) - \Delta_{\Re}(\boldsymbol{r})\tau_y\sigma_y - \Delta_{\Im}(\boldsymbol{r})\tau_x\sigma_y, \tag{20}$$

which is derived from equation (5) by considering $v(\boldsymbol{r}) = v$, $V(\boldsymbol{r}) = 0$ and $m \to +\infty$. In fact, the latter model can be linked to a previous proposal [1]. Notice that I permitted a particle–hole asymmetric bulk TI by allowing a finite chemical potential, which additionally ensures that the system resides in class D. Nevertheless, for the rest of the discussion, I will for simplicity set $\mu = 0$. The latter special case, enhances the symmetry of the system leading to the following symmetry class transition D $\to$ BDI, due to the emergence of a chiral symmetry with matrix σ_z, without though affecting our analysis concerning the emergence of MFs. At this point I include a finite supercurrent along the y-axis by considering $\Delta(\boldsymbol{r}) = \Delta(y) = \Delta e^{iJy}$. Furthermore, I assume that Jy is small which allows us to make the approximation $\Delta(y) \simeq \Delta + i\Delta Jy$. Under these assumptions the Hamiltonian becomes

$$\widehat{\mathcal{H}}(\hat{\boldsymbol{p}}, y) = v\left(\hat{p}_x\tau_z\sigma_y - \hat{p}_y\sigma_x\right) - \Delta\tau_y\sigma_y - \Delta Jy\tau_x\sigma_y. \tag{21}$$
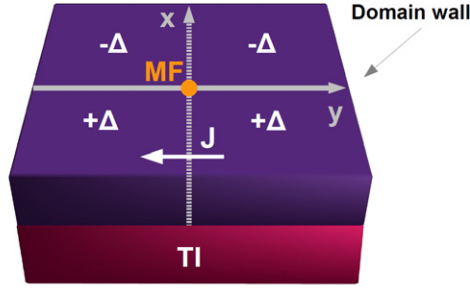
Figure 2. A heterostructure consisting of conventional SCs deposited on top of the surface of a 3D TI. The presence of a superconducting Josephson junction of supercurrent $\boldsymbol{J} = (0, J)$, in combination with a π-superconducting phase domain wall, along $x = 0$, traps a MF at $\boldsymbol{r} = (0, 0)$.

By squaring the BdG Hamiltonian operator, we obtain

$$\widehat{\mathcal{H}}^2(\hat{\boldsymbol{p}}, y) = (v\hat{\boldsymbol{p}})^2 + \Delta^2 + (\Delta J)^2 y^2 + v\hbar \Delta J \tau_x \sigma_z. \tag{22}$$

The above Hamiltonian can be diagonalized in the $y, \hat{p}_y$ space by introducing the eigenstates $|n\rangle$ of a quantum harmonic oscillator with frequency $\omega = 2v\Delta J$ providing

$$\widehat{\mathcal{H}}_n^2(\hat{p}_x) = (v\hat{p}_x)^2 + \Delta^2 + v\hbar \Delta J(2n+1) + v\hbar \Delta J \tau_x \sigma_z. \tag{23}$$

Notice that the presence of the supercurrent leads to confinement parallel to its direction. Since we are interested in the low energy regime, we can restrict to the eigenstates of $\tau_x \sigma_z$ with eigenvalue -1 and $n = 0$. In fact, for the latter eigenstates, the term $v\hbar \Delta J(2n+1) + v\hbar \Delta J \tau_x \sigma_z$ becomes zero, rendering these solutions as Majorana bound state solutions in the absence of $(v\hat{p}_x)^2 + \Delta^2$. With this in mind, I project the following part $v\hat{p}_x \tau_z \sigma_y - \Delta \tau_y \sigma_y$ of equation (21) onto these degenerate lowest energy states, leading to the effective Hamiltonian:

$$\widehat{\mathcal{H}}_{\text{eff}}(\hat{p}_x) = v\hat{p}_x \kappa_y + \Delta \kappa_x, \tag{24}$$

where $\boldsymbol{\kappa}$ correspond to Pauli matrices defined in the truncated basis spanned by the Majorana bound states $|n = 0; \tau_x = -1; \sigma_z = +1\rangle$ and $|n = 0; \tau_x = +1; \sigma_z = -1\rangle$. The latter results are in absolute agreement with the SC–TI–SC heterostructure model considered in [1] and related studies concerning graphene-based hybrid devices [54], following a different approach. Fu and Kane [1], considered a tri-junction of SC–TI–SC systems in order to implement a C_3 vortex at the meeting point which can host a MF. In fact, the SC–TI–SC setup has been recently under experimental investigation [3] revealing possible signatures of MFs. Here, for the detection of MFs, I propose the situation of a π-phase domain wall for the SC gap Δ along the x-axis (figure 2), in analogy to the Jackiw–Rebbi model [55]. However, in the present case the bound states will be of the Majorana type. Note that the equivalent description of the SC–TI–SC heterostructure proposed in [1], using supercurrents as in the present discussion, had not been so far realized, leaving alternative accessible MF setups unexplored. According to the analysis above, a prominent system for hosting MFs is a quasi-1D Rashba semiconductor in proximity to a conventional SC. As I demonstrate in the next paragraph, the presence of a Josephson current flow parallel to the direction where confinement is imposed, will lead to the appearance of edge MFs.
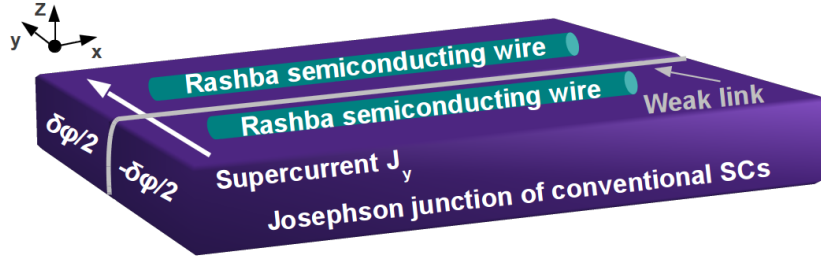
Figure 3. A heterostructure consisting of two coupled single channel wires deposited on top of two conventional SCs interfaced by a weak link permitting the flow of a Josephson current. The supercurrent flow is directed transversely to the wires' axis and is sufficient to generate edge MFs that are 'shared' by the two wires.

6.2. TSC in a heterostructure consisting of two coupled Rashba semiconducting wires and conventional SCs

In this subsection I will focus on quasi-1D Rashba semiconducting platforms. Due to the quasi-1D character of the system, a finite number of channels are generally allowed, which should be taken into full consideration for the MF analysis. Nevertheless, in order to demonstrate the possibility of MFs, based solely on supercurrents, I will here consider the simplest example of a quasi-1D Rashba semiconductor, which consists of two coupled single channel wires (figure 3). Note that double-wire setups [56] have been recently considered in the context of $\mathcal{T}$-invariant TSCs. However, in our case $\mathcal{T}$ will be broken. The relevant Hamiltonian reads

$$\mathcal{H} = \int \mathrm{d}x \sum_{n=\pm} \left\{ \hat{\psi}_n^\dagger(x) \left(\frac{\hat{p}_x^2}{2m} - \mu + v\hat{p}_x \sigma_y \right) \hat{\psi}_n(x) + \left[\Delta e^{ni\frac{\delta\varphi}{2}} \psi_{\uparrow,n}^\dagger(x)\psi_{\downarrow,n}^\dagger(x) + \mathrm{h.c.} \right] \right\}$$

$$+ \int \mathrm{d}x \left\{ t_\perp \hat{\psi}_+^\dagger(x)\hat{\psi}_-(x) + \mathrm{i}V_\perp \hat{\psi}_+^\dagger(x)\sigma_x \hat{\psi}_-(x) + \Delta_\perp \left[\psi_{\uparrow,+}^\dagger(x)\psi_{\downarrow,-}^\dagger(x) \right. \right.$$

$$\left. \left. + \psi_{\uparrow,-}^\dagger(x)\psi_{\downarrow,+}^\dagger(x) \right] + \mathrm{h.c.} \right\}, \tag{25}$$

where $n = \pm$ labels the two parallel single-channel wires placed at distance L_y, while $t_\perp$, $V_\perp$, Δ and $\Delta_\perp$ correspond to inter-wire hopping, inter-wire spin–orbit coupling, intra-wire superconductivity and inter-wire superconductivity, respectively. Moreover, I also introduced a finite supercurrent $J_y \sim \delta\varphi$ flowing from one wire to the other, by incorporating a phase in the intra-wire superconducting gap that has an opposite sign on the two wires. Notice that the inter-wire superconducting term is unaffected by the presence of the supercurrent for the particular direction of flow. For a compact description, I will introduce the spinor

$$\widehat{\Psi}^\dagger(x) = \left(\psi_{\uparrow,+}^\dagger(x), \psi_{\downarrow,+}^\dagger(x), \psi_{\uparrow,-}^\dagger(x), \psi_{\downarrow,-}^\dagger(x), \psi_{\uparrow,+}(x), \psi_{\downarrow,+}(x), \psi_{\uparrow,-}(x), \psi_{\downarrow,-}(x) \right), \tag{26}$$

and additionally employ the κ Pauli matrices that act on the sub-space spanned by the two wire indices $n = \pm$. The BdG Hamiltonian of equation (25) reads

$$\widehat{\mathcal{H}}(\hat{p}_x) = \left(\frac{\hat{p}_x^2}{2m} - \mu \right) \tau_z + t_\perp \tau_z \kappa_x + v\hat{p}_x \tau_z \sigma_y - V_\perp \kappa_y \sigma_x - \Delta e^{\mathrm{i}\frac{\delta\varphi}{2}\tau_z\kappa_z} \tau_y \sigma_y - \Delta_\perp \tau_y \kappa_x \sigma_y. \tag{27}$$

It is straightforward to confirm that the above Hamiltonian is characterized by a chiral symmetry with matrix $\tau_x \kappa_x$ and a concomitant generalized time-reversal symmetry $\Theta = \kappa_x \mathcal{K}$. Due to the property $\Theta^2 = I$, the system resides in class BDI which in 1D is characterized by a $\mathbb{Z}$ topological invariant, allowing an integer number of topologically protected MFs per edge [21, 57]. For the rest I will consider $\mu = 0$ which can be always experimentally achieved by properly gating the device and does not affect our analysis. It is instructive to study the energy spectrum for $p_x = 0$ when the supercurrent is zero, which reads

$$E_{\delta\varphi=0}(p_x = 0) = \pm\sqrt{t_\perp^2 + \left(\Delta_\perp \pm \sqrt{V_\perp^2 + \Delta^2}\right)^2}. \tag{28}$$

We observe that the spectrum is two-fold degenerate and the only possibility for a gap closing at $p_x = 0$, which would imply the presence of MFs, can occur only if $t_\perp = 0$ and $\Delta_\perp = \sqrt{V_\perp^2 + \Delta^2}$. However, even if we consider $t_\perp = 0$, for every realistic case $\Delta > \Delta_\perp$. Consequently, in the absence of a supercurrent, the system cannot support MFs. In order to shed light on how the presence of a finite supercurrent can lead to MFs, I will perform a gauge transformation, $\widehat{\mathcal{H}}'(\hat{p}_x) \equiv e^{-i\frac{\delta\varphi}{4}\tau_z\kappa_z}\widehat{\mathcal{H}}(\hat{p}_x)e^{i\frac{\delta\varphi}{4}\tau_z\kappa_z}$, in order to remove the superconducting phase and obtain an expression similar to equation (6). Furthermore, I will consider $\delta\varphi = \pi - 2\epsilon$ where ϵ is considered small and I will keep terms linear in ϵ. Under these conditions, the Hamiltonian of equation (27) becomes

$$\widehat{\mathcal{H}}'(\hat{p}_x) = \frac{\hat{p}_x^2}{2m}\tau_z + t_\perp \kappa_y + \epsilon t_\perp \tau_z \kappa_x + v\hat{p}_x \tau_z \sigma_y + V_\perp \tau_z \kappa_x \sigma_x - \epsilon V_\perp \kappa_y \sigma_x - \Delta \tau_y \sigma_y - \Delta_\perp \tau_y \kappa_x \sigma_y. \tag{29}$$

Notice that in the presence of a supercurrent for which $\epsilon = 0$, the inter-wire spin–orbit coupling term $V_\perp \kappa_y \sigma_x$ is converted completely into an inter-wire Zeeman term $V_\perp \tau_z \kappa_x \sigma_x$, which is polarized perpendicular to the intra-wire spin–orbit coupling term $v\hat{p}_x \tau_z \sigma_y$ and is crucial for the appearance of MFs in this double-wire setup. For $\epsilon = 0$, the reconstructed energy spectrum for $p_x = 0$ reads

$$E_{\delta\varphi=\pi}(p_x = 0) = \pm\left[\Delta \pm \sqrt{t_\perp^2 + (V_\perp \pm \Delta_\perp)^2}\right]. \tag{30}$$

We observe that there is no degeneracy at $p_x = 0$, which implies that we obtain a single MF per gap closing. For the above spectrum there can be two gap closings at $p_x = 0$ occurring for $\Delta = \sqrt{t_\perp^2 + (V_\perp \pm \Delta_\perp)^2}$ marking the related topological phase boundaries. According to the latter analysis and by additionally calculating the related $\mathbb{Z}$ topological invariant, following [21], I find that the system resides in the topologically non-trivial phase with a single edge MF when the criterion $\sqrt{t_\perp^2 + (V_\perp - \Delta_\perp)^2} < \Delta < \sqrt{t_\perp^2 + (V_\perp + \Delta_\perp)^2}$ is satisfied.

To illustrate the appearance of MFs in a transparent way, I will consider first the following special case $\epsilon = t_\perp = 0$, where the Hamiltonian of equation (29) enjoys a unitary symmetry generated by the matrix κ_x which implies that the two wires are mirror symmetric. The particular mirror symmetry allows for the block diagonalization of the Hamiltonian in the following manner:

$$\widehat{\mathcal{H}}'_\kappa(\hat{p}_x) = \frac{\hat{p}_x^2}{2m}\tau_z + v\hat{p}_x \tau_z \sigma_y + \kappa V_\perp \tau_z \sigma_x - (\Delta + \kappa\Delta_\perp)\tau_y \sigma_y, \tag{31}$$

where $\kappa = \pm 1$ correspond to the eigenvalues of κ_x. The Hamiltonian of each block is essentially the Hamiltonian of the strictly 1D wire TSC discussed in [9, 10], which belongs to class BDI, and supports a single MF per edge when the following criterion is satisfied $V_\perp > \Delta + \kappa\Delta_\perp$.

Consequently, the system resides: **a.** in the topologically trivial phase for $V_\perp < \Delta - \Delta_\perp$, **b.** in the topologically non-trivial phase with a single MF for $|V_\perp - \Delta| < \Delta_\perp$ and **c.** in the topologically non-trivial phase with two MFs for $V_\perp > \Delta + \Delta_\perp$. It is desirable to study the fate of the MFs when the additional chiral symmetry (with matrix τ_x) is broken and a symmetry class transition $BDI \oplus BDI \to BDI$ occurs for the Hamiltonian of equation (31), due to a finite ϵ. For this purpose, I construct the following low energy effective model:

$$\widehat{\mathcal{H}}'_{\text{eff}}(\hat{p}_x) = v\hat{p}_x\rho_y + (V_\perp - \Delta)\eta_z\rho_x - \Delta_\perp\rho_x \tag{32}$$

by projecting the Hamiltonian of equation (31) onto the following gap closing related Majorana bound state solutions:

$$|1\rangle = |\tau_x = +1; \kappa_x = +1; \sigma_z = +1\rangle, \quad |2\rangle = |\tau_x = -1; \kappa_x = +1; \sigma_z = -1\rangle,$$
$$|3\rangle = |\tau_x = -1; \kappa_x = -1; \sigma_z = +1\rangle, \quad |4\rangle = |\tau_x = +1; \kappa_x = -1; \sigma_z = -1\rangle. \tag{33}$$

For the latter procedure I neglected the quadratic in momentum kinetic term $\sim \hat{p}_x^2\tau_z$ since I focus on momenta about $p_x = 0$, while I made use of the η (acting on $\kappa_x = \pm 1$ blocks) and $\boldsymbol{\rho}$ Pauli matrices. The spectrum of the effective model has the following form:

$$E_{\delta\varphi=\pi}(p_x) = \pm\sqrt{(vp_x)^2 + (V_\perp - \Delta \pm \Delta_\perp)^2}, \tag{34}$$

owing the anticipated gap closings at $V_\perp = \Delta \pm \Delta_\perp$, which provide the topological phase boundaries. At this point, I assume that ϵ is small. By adding the corresponding term $-\epsilon V_\perp \kappa_y \sigma_x$ as a perturbation to the above effective model, I finally obtain

$$\widehat{\mathcal{H}}'_{\text{eff}}(\hat{p}_x) = v\hat{p}_x\rho_y + (V_\perp - \Delta)\eta_z\rho_x - \Delta_\perp\rho_x + \epsilon V_\perp\eta_y\rho_x. \tag{35}$$

The inclusion of ϵ modifies crucially the energy spectrum, which now reads

$$E_{\delta\varphi\neq\pi}(p_x) = \pm\sqrt{(vp_x)^2 + \left[\sqrt{(V_\perp - \Delta)^2 + (\epsilon V_\perp)^2} \pm \Delta_\perp\right]^2}. \tag{36}$$

We directly observe that there is only one possible gap closing and consequently only one accessible topological phase supporting a single MF per edge. This can be naturally understood by taking into consideration that the two MFs, previously existing for the topologically non-trivial phase with $V_\perp > \Delta + \Delta_\perp$, hybridize and give rise to a finite energy fermionic solution. Note that the chiral symmetry breaking effects are non-perturbative. In fact, we may observe the effect of an infinitessimal ϵ by rewriting the energy spectrum in the following form:

$$E_{\delta\varphi\neq\pi}(p_x) = \pm\sqrt{(vp_x)^2 + (|V_\perp - \Delta| \pm \Delta_\perp)^2}. \tag{37}$$

We notice that an infinitessimal ϵ will merge the previous three distinct phases of zero, one or two MFs into the following two: (a) a topologically trivial superconducting phase for $|V_\perp - \Delta| > \Delta_\perp$ and (b) a topologically non-trivial phase with a single MF per edge for $|V_\perp - \Delta| < \Delta_\perp$.

In order to make a connection to the related experimental setup, I will consider InSb wires for which we have $v\hbar = 0.2\,\text{eV Å}$, $m = 0.015m_e$ and $\Delta = 250\,\mu\text{eV}$. Furthermore, $t_\perp \simeq \hbar^2/(2mL_y^2)$ and $V_\perp \simeq v\hbar/L_y$. By assuming a constant value for $\Delta_\perp \sim \Delta/5 = 50\,\mu\text{eV}$, equation (30) and also the computation of the related topological invariant provide that the system resides in the topologically non-trivial phase with a single MF per edge for $109 < L_y < 131\,\text{nm}$. In this regime we expect a zero-bias anomaly peak in the tunnelling spectra, which could constitute a sharp signature of MF physics.

7. Examples of topological phases with hidden symmetries

In this section I will demonstrate two examples where unitary or anti-unitary hidden symmetries occur for some of the TSC phases presented in table 2 and demonstrate what are the concomitant modifications of the initial symmetry class.

7.1. Cases I and II in the presence of a single unitary hidden symmetry $\mathcal{O}_u$

Let us now investigate the consequences of the emergence of a 'hidden' symmetry due to the special form of the Rashba spin–orbit coupling term. As a case study I will focus on the topological properties of the following quasi-1D Hamiltonian, introduced in equation (8) of case I:

$$\widehat{\mathcal{H}}(\hat{p}_x, x) = \frac{\hbar}{2m}\left(J_x \hat{p}_x I + J_y \hbar \lambda_y\right) + \left(\frac{\hat{p}_x^2}{2m} - \mu \lambda_z^J\right)\tau_z + \frac{\{v(x), \hat{p}_x\}}{2}\tau_z \sigma_y - v(x)\hbar \lambda_y \sigma_x$$

$$+ \frac{v(x)\hbar}{2}\left(J_x \sigma_y - J_y \tau_z \sigma_x\right) - \Delta \tau_y \sigma_y. \tag{38}$$

Here we will restrict to the special situation where $t_{\pi/Q}v(x) = v(x + \pi/Q) = -v(x)$. We may readily observe in which manner this property leads to an emergent unitary symmetry. The terms of the Hamiltonian that do not contain $v(x)$ are invariant under arbitrary translations and under the action of σ_h, which in our formalism is represented as $\sigma_h = i\tau_z \sigma_z$ in spin-space. Since all the terms with coefficient $v(x)$ are odd under σ_h, the full Hamiltonian is invariant under the action of $\mathcal{O}_u = \sigma_h t_{\pi/Q}$. The appearance of a hidden symmetry $\mathcal{O}_u$ leads to an additional generalized time-reversal symmetry $\widetilde{\Theta} = \mathcal{O}_u \mathcal{T}$ and a concomitant chiral symmetry $\widetilde{\Pi} = \mathcal{O}_u \Pi$, when $\mathbf{J} = \mathbf{0}$. The emergence of $\mathcal{O}_u$ modifies the symmetry class of the system by splitting the symmetry classes DIII and D found earlier, into DIII ⊕ DIII and D ⊕ D, respectively. Note that point group symmetry protected phases are currently under intense investigation [58] and a topological classification of systems with reflection symmetry has also appeared [59]. A simple example for $v(x + \pi/Q) = -v(x)$ is $v(x) = 2v_Q \cos(Qx + \theta)$ with $Q = 2q$. Here, θ is considered pinned to a constant value. The modulated spin–orbit coupling term can be viewed as an unconventional spin triplet density wave [36], similar to the Rashba spin–orbit density wave proposed in [60] as a potential candidate for the so called 'hidden order', which appears in the non-superconducting regime of the phase diagram of the heavy fermion compound URu_2Si_2.

The simultaneous presence of the momentum operator $\hat{p}_x$ and coordinate x does not allow for a direct and transparent inspection of further topological properties of the system. Nonetheless, it is also possible in principle to obtain through some kind of 'deformation' procedure (in the topological sense) a model defined solely in momentum space that shares the same symmetries and topological properties with the original model. In order for this mapping to be meaningful and offer a direct computation of topological invariants, translational symmetry must be somehow restored. The presence of a periodic $v(x) = 2v_Q \cos(Qx + \theta)$ term, leads to the formation of a band structure with a Brillouin zone of length Q since $t_{2\pi/Q}v(x) = v(x)$. The property $t_{\pi/Q}v(x) = -v(x)$ gives rise to a sub-lattice structure that will eventually lead to the two sub-blocks of the Hamiltonian that become relevant in the presence of $\mathcal{O}_u$. Since we are not interested in the full band structure, but mainly in removing the x-dependence of the

Hamiltonian, we may expand the field operator in the following fashion:

$$\hat{\psi}(x) \simeq e^{+iqx}\hat{\psi}_{+q}(x) + e^{-iqx}\hat{\psi}_{-q}(x), \tag{39}$$

where $\hat{\psi}_{\pm q}(x)$ are slowly varying fields leading to the Hamiltonian

$$\begin{aligned}
\widehat{\mathcal{H}}_q(\hat{p}_x) &= \frac{\hbar}{2m}\left(J_x\hat{p}_x I + J_y\hbar\lambda_y\right) + \frac{\hbar}{2}\tilde{v}J_x\rho_z + \left[\frac{\hat{p}_x^2}{2m} + \frac{(\hbar q)^2}{2m} - \mu\lambda_z^J\right]\tau_z + \tilde{v}\hat{p}_x\tau_z\rho_z \\
&\quad + v_Q\hat{p}_x\left(\cos\theta\,\tau_z\rho_x\sigma_y - \sin\theta\,\tau_z\rho_y\sigma_y\right) - v_Q\hbar\left(\cos\theta\,\rho_x\lambda_y\sigma_x - \sin\theta\,\rho_y\lambda_y\sigma_x\right) \\
&\quad + \frac{v_Q\hbar}{2}J_x\left(\cos\theta\,\rho_x\sigma_y - \sin\theta\,\rho_y\sigma_y\right) - \frac{v_Q\hbar}{2}J_y\left(\cos\theta\,\tau_z\rho_x\sigma_x - \sin\theta\,\tau_z\rho_y\sigma_x\right) \\
&\quad - \Delta\tau_y\sigma_y, \tag{40}
\end{aligned}$$

with $\tilde{v} = \hbar q/m$. The above Hamiltonian acts on the enlarged spinor

$$\widehat{\Psi}_q^\dagger(x) = \left(\psi_{+q\uparrow}^\dagger(x), \psi_{+q\downarrow}^\dagger(x), \psi_{-q\uparrow}^\dagger(x), \psi_{-q\downarrow}^\dagger(x), \psi_{-q\uparrow}(x), \psi_{-q\downarrow}(x), \psi_{+q\uparrow}(x), \psi_{+q\downarrow}(x)\right), \tag{41}$$

with the $\boldsymbol{\rho}$ Pauli matrices acting on $\pm q$ space. Notice that terms with ρ_x or ρ_y carry momentum Q. By expanding the field operator in this manner, we managed to end up with a coordinate independent Hamiltonian. This approximation allows us to readily study topological aspects in momentum space which for the specific case is an easier task compared to the required analysis in coordinate space. Nonetheless, it is not *a priori* ensured that the coordinate and momentum pictures are topologically equivalent. If they do, this approximation constitutes a suitable deformation procedure for mapping x to k_x space topology.

In order to confirm if these systems belong to the same symmetry class, we have to study the emerging symmetries for the latter model. In this basis the expression for the generalized time-reversal symmetry operator simplifies to $\Theta = i\sigma_y\mathcal{K} = i\rho_x\sigma_y\mathcal{K}'$, where $\mathcal{K}'$ is a complex conjugation operator not acting on Q or q. The presence of ρ_x effects complex conjugation operation $\mathcal{K}$ in q space, since $q \to -q$ is equivalent to $\mathcal{K} = \rho_x\mathcal{K}'$. Furthermore, within the specific framework $t_{\pi/Q} = -i\rho_z$. Notice that $(-i\rho_z)^2 = -I$, i.e. similar to the behaviour of rotation operators for a spin-$1/2$. This is a direct consequence of the fact that the spinor contains the wave-vector q which is half of the wave-vector $Q = 2q$. We may directly confirm that $[\widehat{\mathcal{H}}_q(\hat{p}_x), \sigma_h t_{\pi/Q}] \equiv [\widehat{\mathcal{H}}_q(\hat{p}_x), \tau_z\rho_z\sigma_z] = 0$. When $\boldsymbol{J} = \boldsymbol{0}$, the Hamiltonian is invariant under Θ and the presence of $\mathcal{O}_u = \sigma_h t_{\pi/Q}$ leads to the additional time-reversal symmetry $\widetilde{\Theta} = \mathcal{O}_u\Theta = i\tau_z\rho_y\sigma_x\mathcal{K}'$. The emerging chiral symmetries for this model read $\Pi = \tau_x\sigma_y$ and $\widetilde{\Pi} = \tau_y\rho_z\sigma_x$. As expected, in this case the system belongs to the symmetry class DIII $\oplus$ DIII. Furthermore, if $\boldsymbol{J} \neq \boldsymbol{0}$ then Θ is broken and the system transits to the symmetry class D $\oplus$ D. To explicitly demonstrate the sub-block structure of the Hamiltonian and the direct sum of symmetry classes, I effect the unitary transformation

$$\Lambda = \frac{I + \rho_z\sigma_z}{2} + \tau_x\frac{I - \rho_z\sigma_z}{2}, \tag{42}$$

which transforms the Hamiltonian as follows $\widehat{\mathcal{H}}_q^{\mathrm{rot}}(\hat{p}_x) = \Lambda^\dagger\widehat{\mathcal{H}}_q(\hat{p}_x)\Lambda$. This particular unitary transformation block diagonalizes the matrix $\tau_z\rho_z\sigma_z$, representing the hidden symmetry operation $\mathcal{O}_u$, into $\Lambda^\dagger\tau_z\rho_z\sigma_z\Lambda = \tau_z$. The transformed Hamiltonian is block diagonal and can

be labelled by the eigenvalues of τ_z, $\tau = \pm 1$, yielding

$$\widehat{\mathcal{H}}_{q,\tau}^{\text{rot}}(\hat{p}_x) = \frac{\hbar}{2m}\left(J_x \hat{p}_x + J_y \hbar \lambda_y\right) I + \frac{\hbar}{2}\tilde{v} J_x \rho_z + \tau \left[\frac{\hat{p}_x^2}{2m} + \frac{(\hbar q)^2}{2m} - \mu \lambda_z^J\right]\rho_z \sigma_z + \tau \tilde{v}\hat{p}_x \sigma_z$$

$$+ v_Q \left(\tau \hat{p}_x \cos\theta + \hbar \lambda_y \sin\theta\right)\rho_y \sigma_x + v_Q \left(\tau \hat{p}_x \sin\theta - \hbar \lambda_y \cos\theta\right)\rho_x \sigma_x$$

$$+ \frac{v_Q \hbar}{2}\left[\left(J_x \cos\theta + \tau J_y \sin\theta\right)\rho_x \sigma_y - \left(J_x \sin\theta - \tau J_y \cos\theta\right)\rho_y \sigma_y\right] + \tau \Delta \rho_z \sigma_x. \quad (43)$$

I have to remark that the above topological classification conclusions hold for a bulk system. In order to observe the two sets of edge MFs one must introduce boundaries that preserve the $\mathcal{O}_u$ symmetry. The usual method followed in order to investigate the bulk-boundary correspondence of a translationally invariant topologically non-trivial system, is to consider an infinite well potential. In the present case the preservation of $\mathcal{O}_u$ requires a specific behaviour under the translation operation $t_{\pi/Q}$. As long as the approximation of equation (39) is well justified and an infinitely steep boundary potential is imposed, the system is characterized by an emergent translational invariance and the two sets of edge MFs should manifestly appear. However, if the boundary potential $V_b(x)$ is not infinitely steep but develops gradually within a certain region l, then the preservation of the $\mathcal{O}_u$ symmetry depends crucially on the wave-vector $q_b \sim 1/l$. If q_b is comparable to q, then the Fourier components V_{q_b} have to be included in the bulk Hamiltonian of equation (40), contributing with terms proportional to $\tau_z \rho_x$, ρ_x, $\tau_z \rho_y$ and ρ_y that break the hidden symmetry. In this case, we may only observe only a single set of edge MFs.

Nonetheless, the situation discussed here does not only constitute an example of mere academic interest, even if in the case where boundary effects can break the hidden symmetry. Although the presence of protected boundary modes [4, 61] is considered to be the hallmark of topologically non-trivial phases, it does not constitute the unique route for diagnosing topological order. In fact, fingerprints of topological non-trivial phases can be also found in manifestations of the bulk system. Consequently, we can obtain information concerning the presence of the 'hidden' symmetry irrespective of the presence of boundaries. One example is the polar Kerr effect [62] that characterizes class D chiral p-wave SCs. This experiment can provide a direct evidence of topological order by solely probing the bulk response. Similar chiral phenomena emerge in non-superconducting systems. In the latter, apart from a similar polar Kerr effect [38, 63], an anomalous thermoelectric Nernst response [39, 64] and a topological Meissner effect [40] constitute additional smoking gun signatures of quantum anomalous Hall phases (class A). In fact, topological response survives also in finite temperatures, though exhibiting no quantization phenomena. Evenmore, the bulk magnetic response [65] of a quantum spin Hall insulator (class AII) can provide alternative routes for confirming the transition to the topologically non-trivial phase.

7.2. Cases III and IV with a single anti-unitary hidden symmetry $\mathcal{O}_a$

Here I will investigate the consequences of the emergence of an anti-unitary hidden symmetry $\mathcal{O}_a$ on the symmetry class of the 1D model of equation (15) that was obtained for cases III and IV. In this way I will be in a position to make a connection to previous studies [26, 27]. The Hamiltonian of equation (15) for $J_x = 0$, has the following form:

$$\widehat{\mathcal{H}}(\hat{p}_x, x) = \left(\frac{\hat{p}_x^2}{2m} - \mu\right)\tau_z - \boldsymbol{M}(x) \cdot \left(\tau_z \sigma_x, \sigma_y, \tau_z \sigma_z\right) - \Delta \tau_y \sigma_y. \quad (44)$$
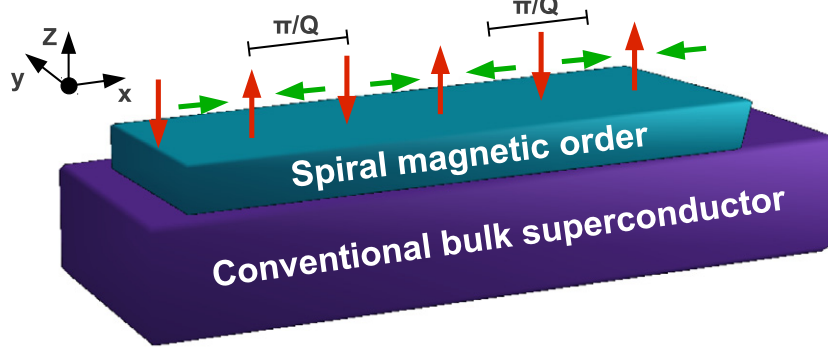
Figure 4. Engineered topological SC consisting of a metal with spin-spiral magnetic order $\boldsymbol{M}(x) = (2M_x^Q\cos Qx, 0, -2M_z^Q\sin Qx)$ placed on top of a bulk conventional SC. The magnetic order is invariant under the combined action of time-reversal symmetry $\mathcal{T}$ followed by a π/Q translation operation, $t_{\pi/Q}$. The presence of the anti-unitary hidden symmetry $\mathcal{O}_a = t_{\pi/Q}\mathcal{T}$ leads to the class BDI⊕BDI, compared to class BDI when it is absent.

First I will focus on the case III, which belongs to class BDI with $\Theta = \mathcal{K}$, if $\boldsymbol{M}(x)$ is random and $M_y(x) = 0$. I demonstrate that the topological properties of the system change with the emergence of a hidden symmetry. I now assume that $t_{\pi/Q}\boldsymbol{M}(x) = \boldsymbol{M}(x + \pi/Q) = -\boldsymbol{M}(x)$. For this special case, the Hamiltonian is invariant under the anti-unitary hidden symmetry $\mathcal{O}_a = t_{\pi/Q}\mathcal{T}$. Since $t_{\pi/Q}$ is unitary and $\mathcal{T}$ anti-unitary, the particular symmetry constitutes an additional generalized time-reversal symmetry $\widetilde{\Theta} = \mathcal{O}_a$. In order to gain more insight, I will consider the simple spin-spiral magnetization profile $M_x(x) = 2M_x^Q\cos Qx$ and $M_z(x) = -2M_z^Q\sin Qx$ which is depicted in figure 4. Prior studies [26, 27] have focused on the special case $M_x^Q = M_z^Q$. By expanding the field operator as in equation (39) we obtain

$$\widehat{\mathcal{H}}(\hat{p}_x) = \left[\frac{\hat{p}_x^2}{2m} + \frac{(\hbar q)^2}{2m} - \mu\right]\tau_z + \tilde{v}\hat{p}_x\tau_z\rho_z - M_x^Q\tau_z\rho_x\sigma_x + M_z^Q\tau_z\rho_y\sigma_z - \Delta\tau_y\sigma_y. \tag{45}$$

Within this framework we have $\Theta = \mathcal{K} = \rho_x\mathcal{K}'$ and $\widetilde{\Theta} = \mathcal{O}_a = t_{\pi/Q}\mathcal{T} = -i\rho_z i\sigma_y\mathcal{K} = -i\rho_z i\sigma_y\rho_x\mathcal{K}' = i\rho_y\sigma_y\mathcal{K}'$. Remember that $\mathcal{K}'$ does not act on q and Q. We readily observe that for both generalized time-reversal symmetries we have $\Theta^2 = \widetilde{\Theta}^2 = +I$ leading to the symmetry class BDI⊕BDI. Note that in [26, 27] it was shown that, up to a spatially dependent unitary transformation, the model of equation (44) is equivalent to the MF-wire model of equation (18) with the latter belonging to the symmetry class BDI. However, as we showed here the particular system in the general case $M_x^Q \neq M_z^Q$ belongs to class BDI ⊕ BDI. It is straightforward to demonstrate that the two pictures agree with each other. By performing the transformation $\widehat{\mathcal{H}}^{\mathrm{rot}}(\hat{p}_x) = \Lambda^\dagger\widehat{\mathcal{H}}^{\mathrm{rot}}(\hat{p}_x)\Lambda$ with $\Lambda = (\rho_z\sigma_z + \sigma_y)(\rho_y + \rho_z)/2$ we obtain

$$\widehat{\mathcal{H}}^{\mathrm{rot}}(\hat{p}_x) = \left[\frac{\hat{p}_x^2}{2m} + \frac{(\hbar q)^2}{2m} - \mu\right]\tau_z + \tilde{v}\hat{p}_x\tau_z\rho_y + M_x^Q\tau_z\rho_z - M_z^Q\tau_z\rho_z\sigma_z - \Delta\tau_y\rho_y\sigma_z. \tag{46}$$

As anticipated, the above Hamiltonian is block diagonal and if we introduce the eigenstates $\sigma = \pm 1$ of σ_z in the rotated frame, we obtain

$$\widehat{\mathcal{H}}_\sigma^{\mathrm{rot}}(\hat{p}_x) = \left[\frac{\hat{p}_x^2}{2m} + \frac{(\hbar q)^2}{2m} - \mu\right]\tau_z + \tilde{v}\hat{p}_x\tau_z\rho_y + \left(M_x^Q - \sigma M_z^Q\right)\tau_z\rho_z - \sigma\Delta\tau_y\rho_y. \tag{47}$$
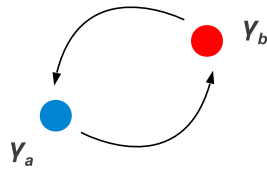
Figure 5. Exchanging MFs in real space leads to a protected single topological qubit rotation termed braiding. In qubit space, this corresponds to a gate operation where the qubit states pick up a relative $\pi/2$ phase.

Remarkably, each of the above block Hamiltonians is identical to the MF-wire Hamiltonian of equation (18) with effective chemical potential $\mu - (\hbar q)^2/2m$, spin–orbit coupling strength $\tilde{v}$, Zeeman field $M_x^Q - \sigma M_z^Q$ and superconducting order parameter $\sigma \Delta$. Each of the blocks will be in the topologically non-trivial phase when the criterion

$$|M_x^Q - \sigma M_z^Q| > \sqrt{\left[\mu - (\hbar q)^2/2m\right]^2 + \Delta^2} \tag{48}$$

is satisfied in complete analogy to equation (19). We observe that the two sub-systems are not necessarily in the topologically non-trivial phase, at the same time. Evenmore, if we consider $M_x^Q = M_z^Q$ as in prior studies [26, 27], only one of the sub-systems can be in the topologically non-trivial phase. In this case, the system effectively behaves as a class BDI TSC and this is in accordance with the previous analytical findings. Note that as long as the translationally invariant Hamiltonian is a good approximation and the boundary potential builds up spatially within a length much smaller that $1/q$, the hidden symmetry will be preserved and the multiple edge MFs are expected to be observed when $M_x^Q \neq M_z^Q$.

8. New topological quantum computing perspectives in a TSC with unitary discrete symmetries

For the cases that we considered in this work, hidden symmetry involved a specific behaviour under translations. However, this type of symmetry is fragile and can be completely broken when boundaries are introduced. Nevertheless, one could look for alternative, robust and tunable, hidden symmetries that are related to some internal degree of freedom such as a valley, orbital or band index.

Let us now discuss new routes that open up for TQC when we consider the additional presence of a hidden unitary discrete symmetry $\mathcal{O}_\mathrm{u}$. Generally, two edge MFs γ_a and γ_b combine into a zero-energy fermion $d = (\gamma_\mathrm{a} + \mathrm{i}\gamma_\mathrm{b})/\sqrt{2}$ that leads to a doubly degenerate ground state $|1\rangle$ and $|0\rangle$. These two states correspond to many-body ground states where the zero-energy fermion is occupied or not, respectively. The Hilbert space spanned by these two degenerate states defines a topological qubit which is in principle [13] protected by decoherence due to the non-local binding of the MFs. The fundamental and in fact the only allowed topologically protected single qubit operation which we may perform is called braiding [11, 12] and corresponds to exchanging the two MFs in real space figure 5. After braiding is effected the states $|1\rangle$ and $|0\rangle$ become $\mathrm{e}^{\mathrm{i}\pi/4}|1\rangle$ and $\mathrm{e}^{-\mathrm{i}\pi/4}|0\rangle$, picking up a relative $\pi/2$ phase. For a counterclockwise rotation, braiding corresponds to the transformation $\gamma_\mathrm{a} \rightarrow +\gamma_\mathrm{b}$ and $\gamma_\mathrm{b} \rightarrow -\gamma_\mathrm{a}$ while for a clockwise rotation we obtain the inverse transformation $\gamma_\mathrm{a} \rightarrow -\gamma_\mathrm{b}$ and $\gamma_\mathrm{b} \rightarrow +\gamma_\mathrm{a}$ [12].
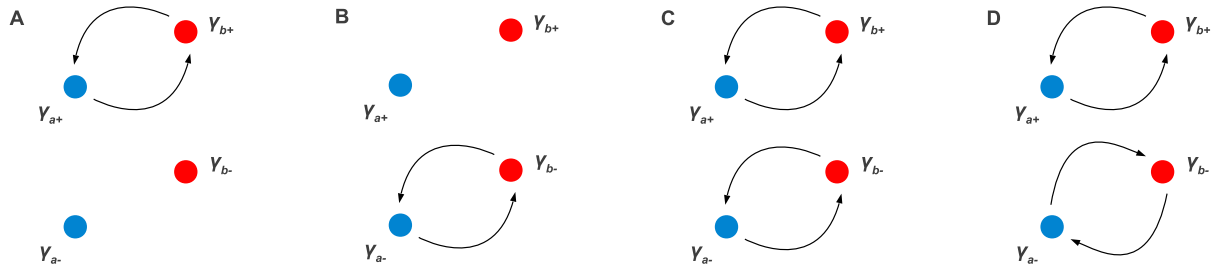
Figure 6. Allowed topologically protected operations for two topological qubits $\pm$ corresponding to the ± 1 eigenvalues of a unitary hidden symmetry operator $\mathcal{O}_u$ satisfying $\mathcal{O}_u^2 = I$. The standard braiding operations A and B describe single qubit operations. C and D correspond to operations in the joint qubit space. In operation C, the $\pm$ pairs of MFs are braided in the same direction while in case D in the opposite.

For a system that supports a single MF per edge, the emergence of a unitary discrete symmetry $\mathcal{O}_u$ with $\mathcal{O}_u^2 = I$, can lead to an additional MF per edge. The two MFs per edge are labelled by the ± 1 eigenstates of $\mathcal{O}_u$, leading to the following four edge MFs $\gamma_{a\pm}$ and $\gamma_{b\pm}$. With the latter, we can define two zero-energy fermions $d_\pm = (\gamma_{a\pm} + i\gamma_{b\pm})/\sqrt{2}$ and two topological qubits with states $\{|1_+\rangle, |0_+\rangle\}$ and $\{|1_-\rangle, |0_-\rangle\}$. The accessible protected non-Abelian operations that we may perform within this four-fold degenerate Hilbert space are restricted by the *simultaneous conservation of fermion parity and* $\mathcal{O}_u$. Essentially, the possible operations are combinations of simultaneous or separate clockwise and counterclockwise braiding operations in each of the topological qubit spaces. Specifically, we have the following four operations:

$$A : \{|1_+\rangle, |0_+\rangle, |1_-\rangle, |0_-\rangle\} \rightarrow \{e^{i\pi/4}|1_+\rangle, e^{-i\pi/4}|0_+\rangle, |1_-\rangle, |0_-\rangle\}, \tag{49}$$

$$B : \{|1_+\rangle, |0_+\rangle, |1_-\rangle, |0_-\rangle\} \rightarrow \{|1_+\rangle, |0_+\rangle, e^{i\pi/4}|1_-\rangle, e^{-i\pi/4}|0_-\rangle\}, \tag{50}$$

$$C : \{|1_+\rangle, |0_+\rangle, |1_-\rangle, |0_-\rangle\} \rightarrow \{e^{i\pi/4}|1_+\rangle, e^{-i\pi/4}|0_+\rangle, e^{i\pi/4}|1_-\rangle, e^{-i\pi/4}|0_-\rangle\}, \tag{51}$$

$$D : \{|1_+\rangle, |0_+\rangle, |1_-\rangle, |0_-\rangle\} \rightarrow \{e^{i\pi/4}|1_+\rangle, e^{-i\pi/4}|0_+\rangle, e^{-i\pi/4}|1_-\rangle, e^{+i\pi/4}|0_-\rangle\}, \tag{52}$$

presented in figure 6. The operations A and B correspond to braiding operations effected only on the $+$ or the $-$ topological qubits. These are single qubit operations. In contrast, if we effect braiding simultaneously in both qubits spaces we have two options. Either the direction of braiding is the same or opposite. These two possible topologically protected operations in the joint qubit space are described by the C and D configurations. The above set of protected operations do not suffice for performing universal TQC due to the Ising nature of the MFs [11, 66]. Nevertheless, the presence of the additional topological qubit on the *same* wire can be useful for performing braiding operations. So far, several methods for performing braiding have been proposed, including networks of topological wires [1, 67] where neighbouring MFs can be controllably coupled in order to perform a MF exchange. In the present case, the additional $\mathcal{O}_u$ protected MFs can constitute a reservoir of MFs that could reduce the number of complementary wires that one needs for performing adiabatic operations using these protocols. In addition, the presence of the extra pair of MFs can be also prominent for creating phase

gate operations. A standard theoretical proposal [11] for implementing a phase gate for two separated MFs, prescribes to bring the MFs to a finite distance in order to let them hybridize into a finite energy fermionic state. Due to the time evolution of the finite energy state, a phase gate operation will be implemented on the topological qubit when the MFs reseparate. In the presence of a hidden symmetry $\mathcal{O}_u$, one does not have to change the distance of the MFs any more. By controllably switching off the hidden symmetry $\mathcal{O}_u$, one hybridizes the two MFs of the same edge, for instance $\gamma_{a\pm}$, so to end up with a single MF. Depending on the details of the hidden symmetry breaking and restoration procedures, one may retrieve a phase gate operation. Of course a detailed investigation of these possibilities is required.

The alternative TQC routes described above depend delicately and crucially on the robustness of this hidden symmetry. As we have already mentioned, it is desirable to find a system that has a hidden symmetry related to a degree of freedom such as a band index. For example, in the case of a two-band topological SC where only intraband matrix elements appear in the Hamiltonian, the system splits into two irreducible sub-systems similarly to the situation described above. As a matter of fact, multiband systems such as the Fe-based high-T_c SCs [68], offer a promising way out. The latter materials are supposed to exhibit intraband superconductivity (usually a four-band [69] or a five-orbital [70] picture is adequate) and consequently we may obtain a number of disconnected sub-systems. If we manage to render each of these superconducting sub-systems topological, we will be in a position to apply the TQC protocols discussed in the previous paragraph. Recently, a proposal concerning topological superconductivity based on iron-based SCs has been put forward [71]. However, in that work an iron-based SC was used to induce superconductivity by proximity effects on a Rashba-semiconductor. Instead, the situation that I envisage involves intrinsic multiband topological superconductivity in the iron pnictide SC itself.

9. Conclusion

I have performed a detailed analysis of the accessible TSC phases that can occur from the combination of inhomogeneous Rashba spin–orbit coupling, magnetic order and superconductivity. By exploring the landscape of the possible topological phases I proposed new systems prominent for realizing MFs, based on Rashba spin–orbit coupling and $\mathcal{T}$ violating superconductivity, without the demand for any kind of magnetic order. Specifically, I explicitly demonstrated the emergence of MFs in a platform consisting of two coupled single channel Rashba semiconducting wires deposited on top of a Josephson junction fabricated by conventional SCs. Moreover, I pinpointed the significance of emergent unitary and anti-unitary hidden symmetries and revealed the topological implications that they lead to. Finally, I discussed alternative TQC pathways that open up in the presence of a unitary hidden symmetry and suggested that Fe-based multiband SCs could be a potential candidate for these implementations.

Acknowledgments

IOP Institute of Physics **Φ** DEUTSCHE PHYSIKALISCHE GESELLSCHAFT

References

[1] Fu L and Kane C L 2008 *Phys. Rev. Lett.* **100** 096407
[2] Mourik V, Zuo K, Frolov S M, Plissard S R, Bakkers E P A M and Kouwenhoven L P 2012 *Science* **336** 6084
   Rokhinson L P, Xinyu L and Furdyna J K 2012 *Nature Phys.* **8** 795
   Deng M T, Yu C L, Huang G Y, Larsson M, Caroff P and Xu H Q 2012 *Nano Lett.* **12** 6414
   Das A, Ronen Y, Most Y, Oreg Y, Heiblum M and Shtrikman H 2012 *Nature Phys.* **8** 887
[3] Williams J R, Bestwick A J, Gallagher P, Hong S S, Cui Y, Bleich A S, Analytis J G, Fisher I R and Goldhaber-
   Gordon D 2012 *Phys. Rev. Lett.* **109** 056803
[4] Hasan M Z and Kane C L 2010 *Rev. Mod. Phys.* **82** 3045
   Qi X L and Zhang S C 2011 *Rev. Mod. Phys.* **83** 1057
[5] Sato M 2003 *Phys. Lett.* B **575** 126
[6] Sato M, Takahashi Y and Fujimoto S 2009 *Phys. Rev. Lett.* **103** 020401
[7] Sau J D, Lutchyn R M, Tewari S and Das Sarma S 2010 *Phys. Rev. Lett.* **104** 040502
[8] Alicea J 2010 *Phys. Rev.* B **81** 125318
[9] Lutchyn R M, Sau J D and Das Sarma S 2010 *Phys. Rev. Lett.* **105** 077001
[10] Oreg Y, Refael G and von Oppen F 2010 *Phys. Rev. Lett.* **105** 177002
[11] Kitaev A Yu 2003 *Ann. Phys.* **303** 2
   Nayak C, Simon S H, Ady S, Freedman M and Das Sarma S 2008 *Rev. Mod. Phys.* **80** 1083
   Ivanov D A 2001 *Phys. Rev. Lett.* **86** 268
[12] Alicea J, Oreg Y, Refael G, von Oppen F and Fisher M P A 2011 *Nature Phys.* **7** 412
[13] Cheng M, Galitski V and Das Sarma S 2011 *Phys. Rev.* B **84** 104529
   Goldstein G and Chamon C 2011 *Phys. Rev.* B **84** 205109
   Budich J C, Walter S and Trauzettel B 2012 *Phys. Rev.* B **85** 121405
   Rainis D and Loss D 2012 *Phys. Rev.* B **85** 174533
   Schmidt M J, Rainis D and Loss D 2012 *Phys. Rev.* B **86** 085414
   Karzig T, Refael G and von Oppen F 2013 arXiv:1305.3626
   Scheurer M S and Shnirman A 2013 *Phys. Rev.* B **88** 064515
[14] Loss D and Di Vincenzo D P 1998 *Phys. Rev.* A **57** 120
   Reilly D J, Taylor J M , Laird E A, Petta J R, Marcus C M, Hanson M P and Gossard A C 2008 *Phys. Rev.
   Lett.* **101** 236803
[15] Makhlin Y, Schön G and Shnirman A 2001 *Rev. Mod. Phys.* **73** 357
   Wellstood F C, Urbina C and Clarke J 1987 *Appl. Phys. Lett.* **50** 772
[16] Kitaev A Yu 2001 *Phys.—Usp.* **44** 131
[17] Fu L and Kane C L 2009 *Phys. Rev.* B **79** 161408
   Jiang L, Pekker D, Alicea J, Refael G, Oreg Y and von Oppen F 2011 *Phys. Rev. Lett.* **107** 236401
[18] Kotetes P, Shnirman A and Schön G 2013 *J. Korean Phys. Soc.* **62** 1558
   Jiang L, Pekker D, Alicea J, Refael G, Oreg Y, Brataas A and von Oppen F 2012 *Phys. Rev.* B **87** 075438
   Meng Q, Shivamoggi V, Hughes T L, Gilbert M J and Vishveshwara S 2012 *Phys. Rev.* B **86** 165110
   Pientka F, Jiang L, Pekker D, Alicea J, Refael G, Oreg Y and von Oppen F 2013 arXiv:1304.7667
[19] San-Jose P, Prada E and Aguado R 2012 *Phys. Rev. Lett.* **108** 257001
   Hützen R, Zazunov A, Braunecker B, Levy Yeyati A and Egger R 2012 *Phys. Rev. Lett.* **109** 166403
   Ojanen T 2012 *Phys. Rev. Lett.* **109** 226804
   Domínguez F, Hassler F and Platero G 2012 *Phys. Rev.* B **86** 140503
   Mai S, Kandelaki E, Volkov A and Efetov K 2013 *Phys. Rev.* B **87** 024507
   Pikulin D I and Nazarov Y V 2012 *Phys. Rev.* B **86** 140504

IOP Institute of Physics   **Φ** DEUTSCHE PHYSIKALISCHE GESELLSCHAFT

Didier N, Gibertini M, Moghaddam A G, König J and Fazio R 2013 *Phys. Rev.* B **88** 024512

Ojanen T 2013 *Phys. Rev.* B **87** 100506

[20] Potter C A and Lee P A 2010 *Phys. Rev. Lett.* **105** 227003

Potter C A and Lee P A 2011 *Phys. Rev.* B **83** 094525

Lutchyn R M, Stanescu T and Das Sarma S 2011 *Phys. Rev. Lett.* **106**

Tewari S, Stanescu T D, Sau J D and Das Sarma S 2012 *Phys. Rev.* B **86** 024504

Reuther J, Alicea J and Yacoby A 2013 *Phys. Rev.* X **3** 031011

Hutasoit J A and Balram A C 2013 *Phys. Rev.* B **88** 075407

[21] Tewari S and Sau J D 2012 *Phys. Rev. Lett.* **109** 150408

[22] Leijnse M and Flensberg K 2011 *Phys. Rev. Lett.* **107** 210502

[23] Lu Y M and Wang Z 2013 *Phys. Rev. Lett.* **110** 096403

Sela E, Altland A and Rosch A 2011 *Phys. Rev.* B **84** 085114

Neupert T, Onoda S and Furusaki A 2010 *Phys. Rev. Lett.* **105** 206404

Chung S B, Zhang H J, Qi X L and Zhang S C 2011 *Phys. Rev.* B **84** 060510

Nersesyan A A and Tsvelik A M 2011 arXiv:1105.5835

[24] Tsvelik A M 2011 arXiv:1106.2996v1

[25] Choy T P, Edge J M, Akhmerov A R and Beenakker C W J 2011 *Phys. Rev.* B **84** 195442

[26] Kjaergaard M, Wölms K and Flensberg K 2012 *Phys. Rev.* B **85** 020503

[27] Martin I and Morpurgo A F 2012 *Phys. Rev.* B **85** 144505

[28] Nadj-Perge S, Drozdov I K, Bernevig B A and Yazdani A 2013 *Phys. Rev.* B **88** 020407(R)

[29] Mizushima T, Sato M and Machida K 2012 *Phys. Rev. Lett.* **109** 165301

Mizushima T and Sato M 2013 *New J. Phys.* **15** 075010

[30] Ramazashvili R 2008 *Phys. Rev. Lett.* **101** 137202

[31] Nandkishore R and Levitov L 2012 *Phys. Rev.* B **82** 115124

[32] Majorana E 1937 *Nuovo Cimento* **5** 171

[33] Wilczek F 2009 *Nature Phys.* **5** 614

[34] Read N and Green D 2000 *Phys. Rev.* B **61** 10267

[35] Michelsen J and Grein R 2012 arXiv:1208.1090

Sau J D, Lutchyn R M, Tewari S and Das Sarma S 2010 *Phys. Rev.* B **82** 094522

Stanescu T D, Sau J D, Lutchyn R M and Das Sarma S 2010 *Phys. Rev.* B **81** 241310

Grein R, Michelsen J and Eschrig M 2012 *J. Phys.: Conf. Ser.* **391** 012149

[36] Nayak C 2000 *Phys. Rev.* B **62** 4880

Thalmeier P 1996 *Z. Phys.* B **100** 387

[37] Hsu C H, Raghu S and Chakravarty S 2011 *Phys. Rev.* B **84** 155111

[38] Tewari S, Zhang C, Yakovenko V M and Das Sarma S 2008 *Phys. Rev. Lett.* **100** 217004

[39] Kotetes P and Varelogiannis G 2010 *Phys. Rev. Lett.* **104** 106404

Zhang C, Tewari S, Yakovenko V M and Das Sarma S 2008 *Phys. Rev.* B **78** 174508

[40] Kotetes P and Varelogiannis G 2008 *Phys. Rev.* B **78** 220509

[41] So T, Fregoso B M, Galitski V and Das Sarma S 2013 *Phys. Rev.* B **87** 014504

Wong C L M and Law K T 2012 *Phys. Rev.* B **86** 184516

[42] Altland A and Zirnbauer M R 1997 *Phys. Rev.* B **55** 1142

[43] Ryu S, Schnyder A, Furusaki A and Ludwig A 2010 *New J. Phys.* **12** 065010

[44] Kitaev A 2009 *AIP Conf. Proc.* **1134** 22

[45] Volovik G E 2003 *The Universe in a Helium Droplet* (Oxford: Clarendon)

[46] Varelogiannis G 2000 *Phys. Rev. Lett* **85** 4172

[47] Tsonis S, Kotetes P, Varelogiannis G and Littlewood P B 2008 *J. Phys.: Condens. Matter* **20** 434234

[48] Aperis A, Varelogiannis G and Littlewood P B 2010 *Phys. Rev. Lett.* **104** 216403

[49] Varelogiannis G 2013 arXiv:1305.2976

[50] Qi X L, Hughes T and Zhang S C 2008 *Phys. Rev.* B **78** 195424

IOP Institute of Physics Φ DEUTSCHE PHYSIKALISCHE GESELLSCHAFT

[51] Fulde P and Ferrell R A 1964 *Phys. Rev.* **135** A550
[52] Larkin A I and Ovchinnikov Y N 1965 *Sov. Phys.—JETP* **20** 762
Agterberg D F and Tsunetsugu H 2008 *Nature Phys.* **4** 639
[53] Liu X J and Lobos A M 2013 *Phys. Rev.* B **87** 060504
Romito A, Alicea J, Refael G and von Oppen F *Phys. Rev.* B **85** 020502
Seradjeh B and Grosfeld E 2011 *Phys. Rev.* B **83** 174521
[54] Titov M and Beenakker C W J 2006 *Phys. Rev.* B **74** 041401
Titov M, Ossipov A and Beenakker C W J 2007 *Phys. Rev.* B **75** 045417
[55] Jackiw R and Rebbi C 1976 *Phys. Rev.* D **13** 3398
[56] Keselman A, Fu L, Stern A and Berg E 2013 *Phys. Rev. Lett.* **111** 116402
Gaidamauskas E, Paaske J and Flensberg K 2013 arXiv:1309.2808
[57] Lutchyn R M and Fisher M P A 2011 *Phys. Rev.* B **84** 214528
[58] Fu L 2011 *Phys. Rev. Lett.* **106** 106802
Fang C, Gilbert M J and Bernevig B A 2012 *Phys. Rev.* B **86** 115112
Jadaun P, Di X, Niu Q and Banerjee S K 2012 arXiv:1208.1472
Ueno Y, Ai Y, Tanaka Y and Sato M 2013 *Phys. Rev. Lett.* **111** 087002
Zhang F, Kane C L and Mele E J 2013 *Phys. Rev. Lett.* **111** 056403
[59] Chiu C K, Hong Y and Ryu S 2013 *Phys. Rev.* B **88** 075142
[60] Das T 2012 *Sci. Rep.* **2** 596
[61] Kane C L and Mele E J 2005 *Phys. Rev. Lett.* **95** 146802
Kane C L and Mele E J 2005 *Phys. Rev. Lett.* **95** 226801
König M, Wiedmann S, Brüne C, Roth A, Buhmann H, Molenkamp L W, Qi X L and Zhang S C 2007 *Science* **318** 766
Roth A, Brüne C, Buhmann H, Molenkamp L W, Maciejko J, Qi X L and Zhang S C 2009 *Science* **325** 294
[62] Kapitulnik A, Xia J, Schemm E and Palevski A 2009 *New J. Phys.* **11** 055060
Lutchyn R M, Nagornykh P and Yakovenko V M 2009 *Phys. Rev.* B **80** 104508
Goryo J 2008 *Phys. Rev.* B **78** 060501
[63] Nandkishore R and Levitov L 2011 *Phys. Rev. Lett.* **107** 097402
[64] Di X, Chang M C and Niu Q 2010 *Rev. Mod. Phys.* **82** 1959
[65] Goryo J and Maeda N 2011 *J. Phys. Soc. Japan* **80** 044707
[66] Bravyi S and Kitaev A 2005 *Phys. Rev.* A **71** 022316
Bravyi S 2006 *Phys. Rev.* A **73** 042313
Sau J D, Tewari S and Das Sarma S 2010 *Phys. Rev.* A **82** 052322
[67] Sau J D, Clarke D J and Tewari S 2011 *Phys. Rev.* B **84** 094505
van Heck B, Akhmerov A R, Hassler F, Burrello M and Beenakker C W J 2012 *New J. Phys.* **14** 035019
Halperin B I, Oreg Y, Ady S, Refael G, Alicea J and von Oppen F 2012 *Phys. Rev.* B **85** 144501
[68] Kamihara Y, Watanabe T, Hirano M and Hosono H 2008 *J. Am. Chem. Soc.* **130** 3296
Singh D J and Du M H 2008 *Phys. Rev. Lett.* **100** 237003
Mazin I I and Schmalian J 2009 *Physica* C **469** 614
[69] Korshunov M M and Eremin I 2008 *Phys. Rev.* B **78** 140509
Aperis A, Kotetes P, Varelogiannis G and Oppeneer P M 2011 *Phys. Rev.* B **83** 092505
[70] Kuroki K, Onari S, Arita R, Usui H, Tanaka Y, Kontani H and Aoki H 2008 *Phys. Rev. Lett.* **101** 087004
[71] Zhang F, Kane C L and Mele E J 2013 *Phys. Rev. Lett.* **111** 056402